Journal of Coastal Research	28	4	903–922	West Palm Beach, Florida	July 2012

Synthesis Study of an Erosion Hot Spot, Ocean Beach, California

Patrick L. Barnard[†], Jeff E. Hansen[†‡], and Li H. Erikson[†]

[†]United States Geological Survey
Pacific Coastal and Marine Science Center
400 Natural Bridges Drive
Santa Cruz, CA 95060, U.S.A.
pbarnard@usgs.gov

[‡]University of California Santa Cruz
Department of Earth and Planetary Sciences
1156 High Street
Santa Cruz, CA 95064, U.S.A.

www.cerf-jcr.org

www.JCRonline.org

ABSTRACT

Barnard, P.L.; Hansen, J.E., and Erikson, L.H., 2012. Synthesis study of an erosion hot spot, Ocean Beach, California (USA). *Journal of Coastal Research,* 28(4), 903–922. West Palm Beach (Florida), ISSN 0749-0208.

A synthesis of multiple coastal morphodynamic research efforts is presented to identify the processes responsible for persistent erosion along a 1-km segment of 7-km-long Ocean Beach in San Francisco, California. The beach is situated adjacent to a major tidal inlet and in the shadow of the ebb-tidal delta at the mouth of San Francisco Bay. Ocean Beach is exposed to a high-energy wave climate and significant alongshore variability in forcing introduced by varying nearshore bathymetry, tidal forcing, and beach morphology (*e.g.,* beach variably backed by seawall, dunes, and bluffs). In addition, significant regional anthropogenic factors have influenced sediment supply and tidal current strength. A variety of techniques were employed to investigate the erosion at Ocean Beach, including historical shoreline and bathymetric analysis, monthly beach topographic surveys, nearshore and regional bathymetric surveys, beach and nearshore grain size analysis, two surf-zone hydrodynamic experiments, four sets of nearshore wave and current experiments, and several numerical modeling approaches. Here, we synthesize the results of 7 years of data collection to lay out the causes of persistent erosion, demonstrating the effectiveness of integrating an array of data sets covering a huge range of spatial scales. The key findings are as follows: anthropogenic influences have reduced sediment supply from San Francisco Bay, leading to pervasive contraction (*i.e.,* both volume and area loss) of the ebb-tidal delta, which in turn reduced the regional grain size and modified wave focusing patterns along Ocean Beach, altering nearshore circulation and sediment transport patterns. In addition, scour associated with an exposed sewage outfall pipe causes a local depression in wave heights, significantly modifying nearshore circulation patterns that have been shown through modeling to be key drivers of persistent erosion in that area.

ADDITIONAL INDEX WORDS: *Erosion, modeling, beach, waves, erosion hot spot.*

INTRODUCTION

Understanding the physical processes driving the persistence of local coastal erosion is key to effective mitigation, particularly in urban areas, where high-value infrastructure is often at risk. In addition to understanding the physical processes occurring directly where erosion is occurring, knowledge of the larger spatial and temporal processes is essential. Examples of important, larger-scale processes include natural and anthropogenic influences on sediment supply and pathways (*e.g.,* Frihy and Komar, 1993; Jabaloy-Sánchez *et al.,* 2010; Slagel and Griggs, 2008), bathymetric change (*e.g.,* Elias and van der Spek, 2006), shoreline and cliff change (*e.g.,* Hapke, Reid, and Richmond, 2009; Jones *et al.,* 2009), tidal currents (*e.g.,* Davis and Barnard, 2003), wave-focusing patterns (*e.g.,* Shi *et al.,* 2011), and wave climate trends (*e.g.,* Allan and Komar, 2006; Ruggiero, Komar, and Allan, 2010). In coastal settings adjacent to river deltas or ebb-tidal deltas, the interaction among sediment supply, wave climate, and tidal currents controls the evolution of the bathymetry (Wright and Coleman, 1972), which in turn exerts a first-order control on the nearshore coastal processes (*e.g.,* Davis and Fox, 1981) and shoreline behavior (*e.g.,* Barnard and Davis, 1999; Davis and Barnard, 2000; El Banna and Frihy, 2009; Fan, Huang, and Zeng, 2006; Mateo and Siringan, 2007).

Erosion "hot spots" are herein defined as local sections of beach—O(100 to 1000) m alongshore—that show persistent multiannual to decadal anomalous erosion or higher erosion rates compared to the adjacent beach (Bridges, 1995; Dean, Liotta, and Simón, 1999; Stauble, 1994). Hot spots have been linked to (1) alongshore-varying nearshore bathymetry, often associated with tidal inlets (*e.g.,* Bruno, Yavary, and Herrington, 1998; Hicks *et al.,* 1999), river mouths (*e.g.,* Barnard and Warrick, 2010), dredge borrow pits (*e.g.,* Benedet and List, 2008), transverse bars (*e.g.,* Hapke *et al.,* 2010; Konicki and Holman, 2000), or bedrock irregularities (*e.g.,* McNinch, 2004), or (2) shadowing effects associated with coastal headlands and structures, such as breakwaters, groins, and jetties, all of which directly interrupt alongshore transport (Kraus and Galgano, 2001).

An erosion hot spot has persisted for decades in the southern reach of Ocean Beach in San Francisco, California, fronting critical wastewater infrastructure for the City of San Francisco. Beach and bluff loss from storms during winter 2009–10 led to $5 million in emergency remediation efforts in the hot-spot area, and continued erosion could lead to significant impacts along this shoreline. Hard structures that impede littoral transport, such as breakwaters, groins, and jetties, are

DOI: 10.2112/JCOASTRES-D-11-00212.1 received 22 November 2011; accepted in revision 21 December 2011.
© Coastal Education & Research Foundation 2012

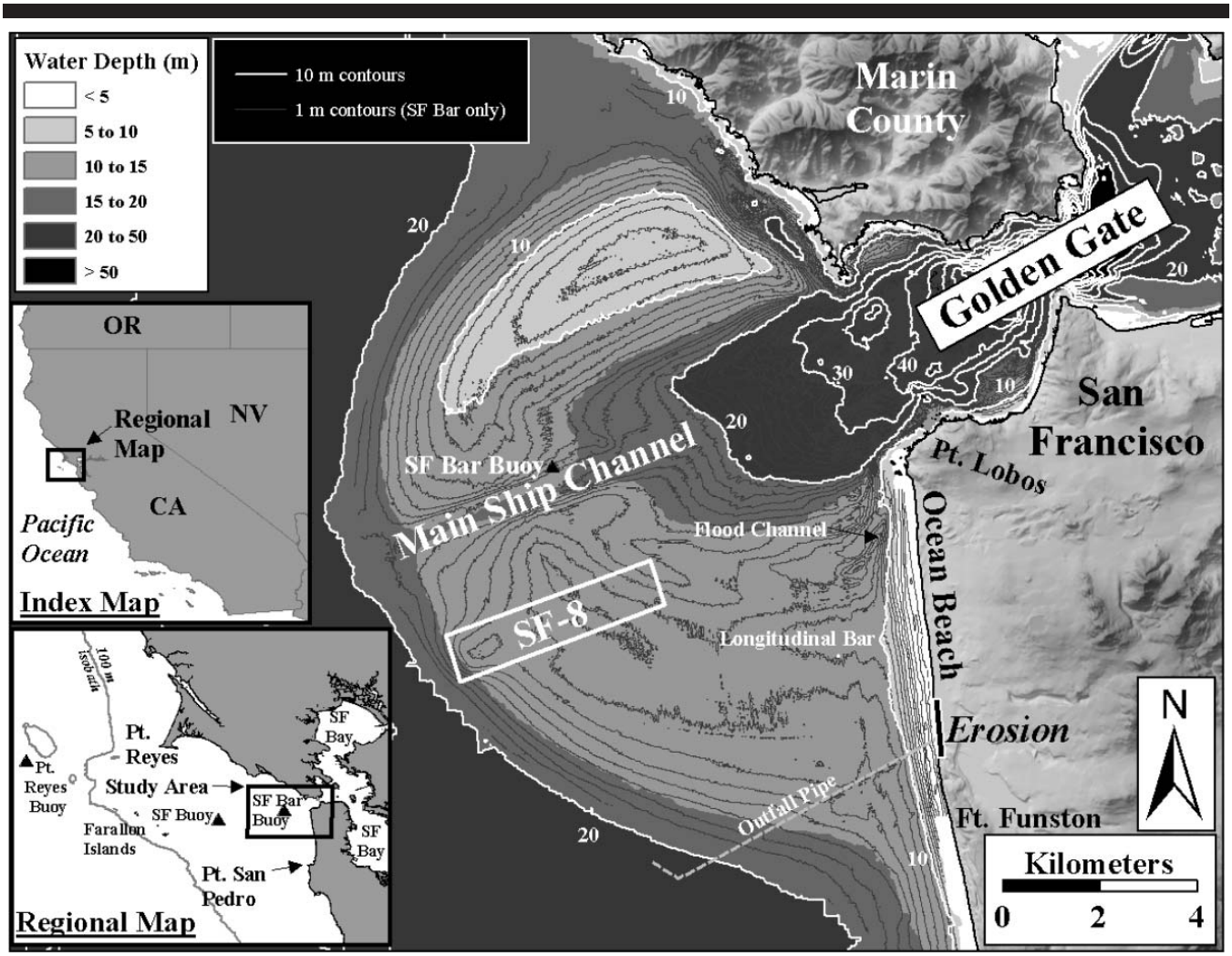

Figure 1. Overview of the study area.

nonexistent along Ocean Beach; thus, alongshore variations in the nearshore bathymetry, as well as tidal and wave forcing associated with natural geography, are expected to be the major contributing factors to the hot-spot erosion. In this paper, we synthesize the findings of a variety of local and regional analyses to describe the primary contributors to persistent erosion in the southern end of Ocean Beach. Our investigation highlights the importance of a comprehensive regional approach to understanding the processes controlling the behavior of a discrete section of coast. Furthermore, this work directly supports key management questions regarding the mitigation of coastal erosion and the protection of valuable infrastructure.

STUDY AREA

Ocean Beach is a 7-km-long, sandy (d_{50} = 0.3 mm) beach located on the U.S. West Coast in the center of the San Francisco Littoral Cell, which extends from Point Reyes in the north to Point San Pedro in the south (Figure 1). Ocean Beach trends north–south along the southern perimeter of the Golden Gate inlet, the sole tidal inlet emptying San Francisco Bay, where tidal currents exceed 2.5 m/s during peak tidal flows in the inlet throat and reach 1.5 and 0.5 m/s at the extreme north and south ends of the beach, respectively (Barnard *et al.,* 2007a). A massive ebb-tidal delta (>150 km^2) is located seaward of the Golden Gate, exerting dominant control on regional wave patterns (Eshleman *et al.,* 2007). Bathymetric features within the ebb-tidal delta that directly influence coastal morphodynamics at Ocean Beach include a 1.5-km-wide longitudinal bar along the southern lobe of the delta that merges with the nearshore in the center of the beach, a flood channel that cuts across the outer surf zone to the north, and a 200-m-wide scour pit associated with an exposed sewage outfall pipe offshore to the south (Figure 1). These features produce irregular alongshore bathymetry and influence physical forcing. The variable nearshore morphology and strong tidal currents cause complex patterns of wave focusing and refraction, alongshore wave height variability (Eshleman *et al.,* 2007), and wave–tidal current interaction.

The regional mean annual deep-water significant wave height H_s is 2.5 m, with a maximum of 9.1 m at the Point Reyes wave

Table 1. *Summary of wave statistics during the study period from April 1, 2004, to March 31, 2010.*

Wave Buoy	Depth (m)	H_s (m) Mean	H_s (m) Max	H_s (m) Min	T_p (s) Mean	T_p (s) Max	D_p (°) Mean
Deep water	550	2.5	9.1	0.6	11.7	25.0	292
Shelf	55	1.9	8.6	0.4	11.3	23.5	279
Bar	15	1.8	6.8	0.4	12.1	25.0	257

buoy (Table 1 and Figure 2; Scripps Institution of Oceanography, 2011). The dissipation of deep-water waves by the shelf reduces H_s by about 25%, although nearshore in 11.5-m water depth in the middle of Ocean Beach, the maximum wave height H_{max} has been measured as more than 10 m due to local focusing (Hansen and Barnard, 2010). Swell typically approaches the region from the NW and W, but S swell can occur during the summer months.

Ocean Beach extends from the rocky headland at Point Lobos to the sandy bluffs of Fort Funston (Figures 1 and 3). The back beach position is variably buttressed by seawalls (2.5 km, northern end and central), dunes (2.2 km, north–central and south–central), revetments or low bluffs (1.0 km, southern end, hot-spot region), and high bluffs (1.3 km, extreme south end). Based on a 150-year study of shoreline change, the southern section of Ocean Beach has a long-term erosion trend (Dallas and Barnard, 2011). Hansen and Barnard (2010) documented accelerated erosion in recent years, culminating in extensive shoreline and bluff retreat observed during the powerful El Niño winter storm season of 2009–10 (Barnard *et al.,* 2011; Barnard, Hoover, and Hansen, 2011) that caused the partial collapse of a major roadway and destruction of a parking lot (Figure 3, upper right). The shoreline of Ocean Beach was extended seaward to accommodate expansion of the City of San Francisco in the early 20th century. At the southern end of Ocean Beach, a nontidal outlet from Lake Merced was filled in and the shoreline was built out to allow construction of the Great Highway in the 1920s (Figure 3, bottom).

METHODS

What follows is a brief summary of the methods employed in this study. For more detailed information, refer to the following references: Barnard *et al.* (2007a, 2007b, 2009); Barnard, Erikson, and Hansen (2009); Barnard and Warrick (2010); Dallas and Barnard (2009, 2011); and Hansen and Barnard (2010). A summary of the data collection locations is displayed in Figure 4.

Beach Mapping and Shoreline Change

Subaerial beach mapping was performed at least monthly at Ocean Beach between 2004 and 2010 using an all-terrain vehicle (ATV) with a real-time kinematic global positioning system (RTK-GPS), with additional pre- and poststorm surveys conducted in the winters of 2005–06, 2006–07, and 2009–10. The vertical uncertainty of the ATV-collected raw data points is typically less than 5 cm, and the maximum mean systematic offset of intersurvey ground control points (raw and gridded) is less than 3 cm (Barnard *et al.,* 2009). Grids are generated from the point data, and both shoreline and volume changes between surveys are calculated. Hansen and Barnard (2010) found a significant correlation between the mean high water (MHW) shoreline position and volume at Ocean Beach. Therefore, we report only MHW shoreline change in this study. Given typical slopes in the region ($\tan\beta = 0.04$), the mean positional uncertainty of a shoreline is about 0.75 m.

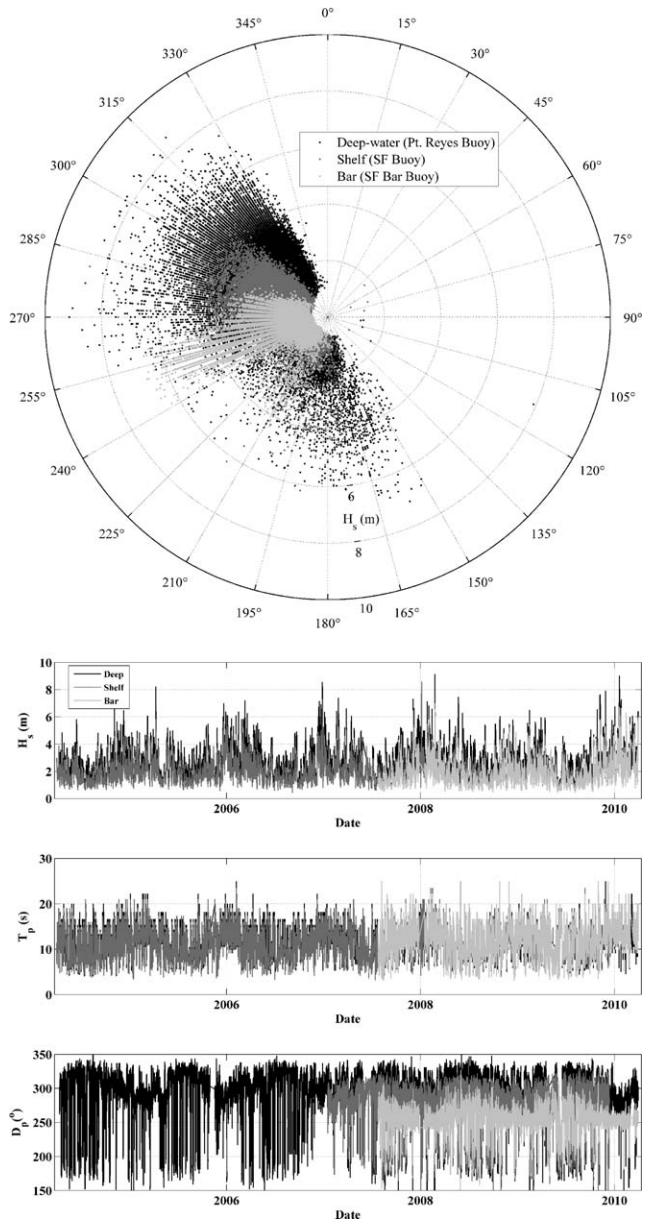

Figure 2. Wave data from the study area collected during the study period from April 1, 2004, to March 31, 2010. Top: Polar plot of wave height and direction for the three wave buoys in the region (see Figure 1 for locations). Bottom: Wave parameters during the study period. The San Francisco buoy (SF Buoy-Shelf) only began reporting directional wave data in January 2007, and the San Francisco bar buoy (SF Bar Buoy) was first deployed in July 2007.

Nearshore Mapping

The coastal profiling system (CPS), a hydrographic surveying system mounted on a personal watercraft (MacMahan, 2001; Ruggiero *et al.,* 2005), was used to perform bathymetric

Figure 3. Erosion at the south end of Ocean Beach. Upper left: View south from the northern end of Ocean Beach. Upper right: Bluff erosion in January 2010 within the erosion hot spot. Bottom: Historical shoreline positions at the southern end of Ocean Beach. The area of critical erosion shown is with the white box (see Figure 1 to reference the location). Lake Merced is pictured to the SE of the hot spot.

surveys along Ocean Beach between 2004 and 2010 approximately quarterly. The CPS collects accurate position and depth data at 10 Hz using RTK-GPS and a single-beam echo sounder to produce bathymetric profiles in areas inaccessible to larger boats. The vertical uncertainty of CPS-collected soundings is typically less than 10 cm, although intrasurvey cross-track comparisons show less than 1-cm mean variability. CPS surveys at Ocean Beach are performed along 18 1.5-km cross-shore and 2 alongshore transects (Figure 4) in water depths of about 1 to 12 m to quantify profile evolution, bar movement, and cross-shore sediment transport.

The mouth of San Francisco Bay (154 km^2) was mapped in 2004–05 using a Reson 8101 multibeam sonar system aboard the *R/V VenTresca* operated by the Sea Floor Mapping Lab at California State University, Monterey Bay. More than 1.2 billion soundings were collected during 44 days of surveying. Horizontal and vertical positional accuracy of this system is typically ± 1 to 2 and ± 0.12 m, respectively. Due to the density of data, gridding error is insignificant; thus, the overall vertical uncertainty is about 12 cm.

Grain Size

Offshore sediment samples were collected annually from 1997 to 2008 at 56 stations at the mouth of San Francisco Bay by the San Francisco Public Utilities Commission (Figure 4). Each sample is a composite of two surface grabs taken at each site using a Smith-McIntyre grab and a 5-cm minimum depth of penetration criterion. The top 2 cm (1997–99) or top 5 cm (2000–09) from the two grabs were combined and homogenized in the field. Grain size was analyzed *via* dry sieving on a shaker table. Silt and clay were individually separated by hydrometer analysis from 1997 to 2004; however, since 2005, they have not

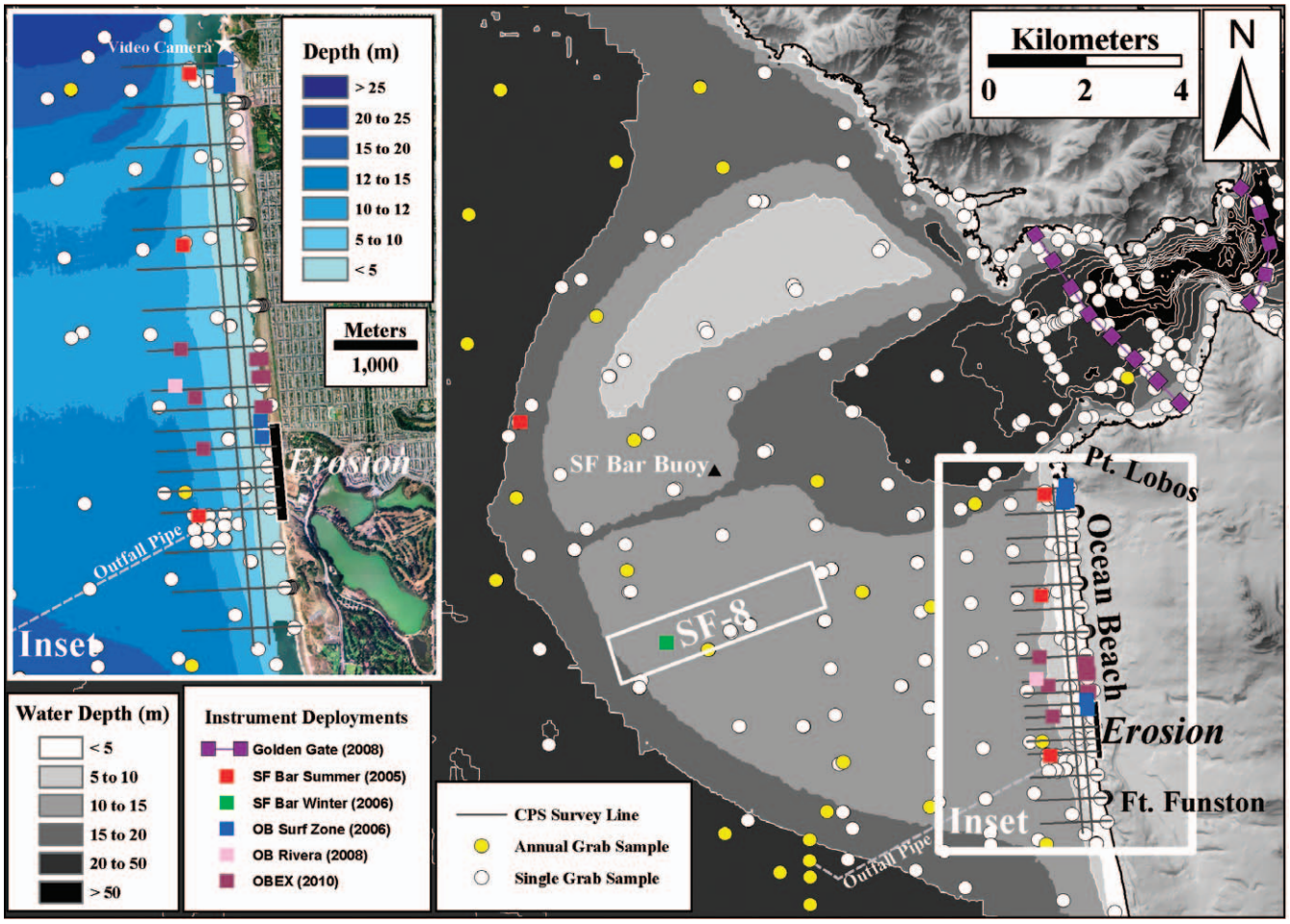

Figure 4. Summary of data collection at Ocean Beach. The main map and the inset include 10- and 1-m bathymetric contours, respectively. For SF Bar Winter, instruments at the northern and southern ends of the beach were colocated with the SF Bar Summer sites and therefore are not shown on the maps.

been separated, so only percent mud was reported. In summer 2005, 91 grab samples were collected from the region (Figure 4), with grain size determined using a settling tube (Gibbs, 1972). In 2008 and 2010, an additional 227 samples were collected, with the results determined by coulter laser.

Oceanographic Instrumentation

Acoustic Doppler current profilers (ADCPs) were deployed during six separate experiments (Table 2 and Figure 4) to gain a better understanding of wave and current variability locally and regionally, as well as provide calibration and validation data sets for numerical models. Additional specific goals of these efforts were to quantify wave transformation across the San Francisco bar (SF Bar Summer and SF Bar Winter in Figure 4), alongshore wave variability nearshore at Ocean Beach (SF Bar Summer, SF Bar Winter, and the Ocean Beach experiment, or OBEX, in Figure 4), and the discharge and total suspended mass flux of sediment across the inlet throat (Golden Gate in Figure 4). Except for the Golden Gate experiment, which utilized a boat-mounted ADCP and cross-channel transects to measure discharge and sediment flux across the inlet throat, all other ADCPs were bottom mounted, were upward looking, and measured both waves and currents. The most extensive instrument deployment was the OBEX (Figure 4), which consisted of three ADCP

Table 2. *Physical process measurements at the mouth of San Francisco Bay and offshore Ocean Beach from 2005 to 2010.*

Experiment	Date	Instruments	Goals/Measurements
SF Bar Summer	Summer 2005	ADCP (4)	Regional summer wave and current variations, model testing
SF Bar Winter	Winter 2006	ADCP (3)	Regional winter wave and current variations, model testing
OB Surf Zone	February 2006	ADCP (6)	Ocean Beach surf zone circulation patterns, model testing
Golden Gate	Winter 2008	ADCP (boat mounted)	Golden Gate discharge/sediment flux, model testing
OB Rivera	Winter 2008	ADCP (1)	Wave conditions on bar peak, model testing
OBEX	Winter 2010	ADCP/ADV (9), pressure sensor (6)	Alongshore wave height and setup variation

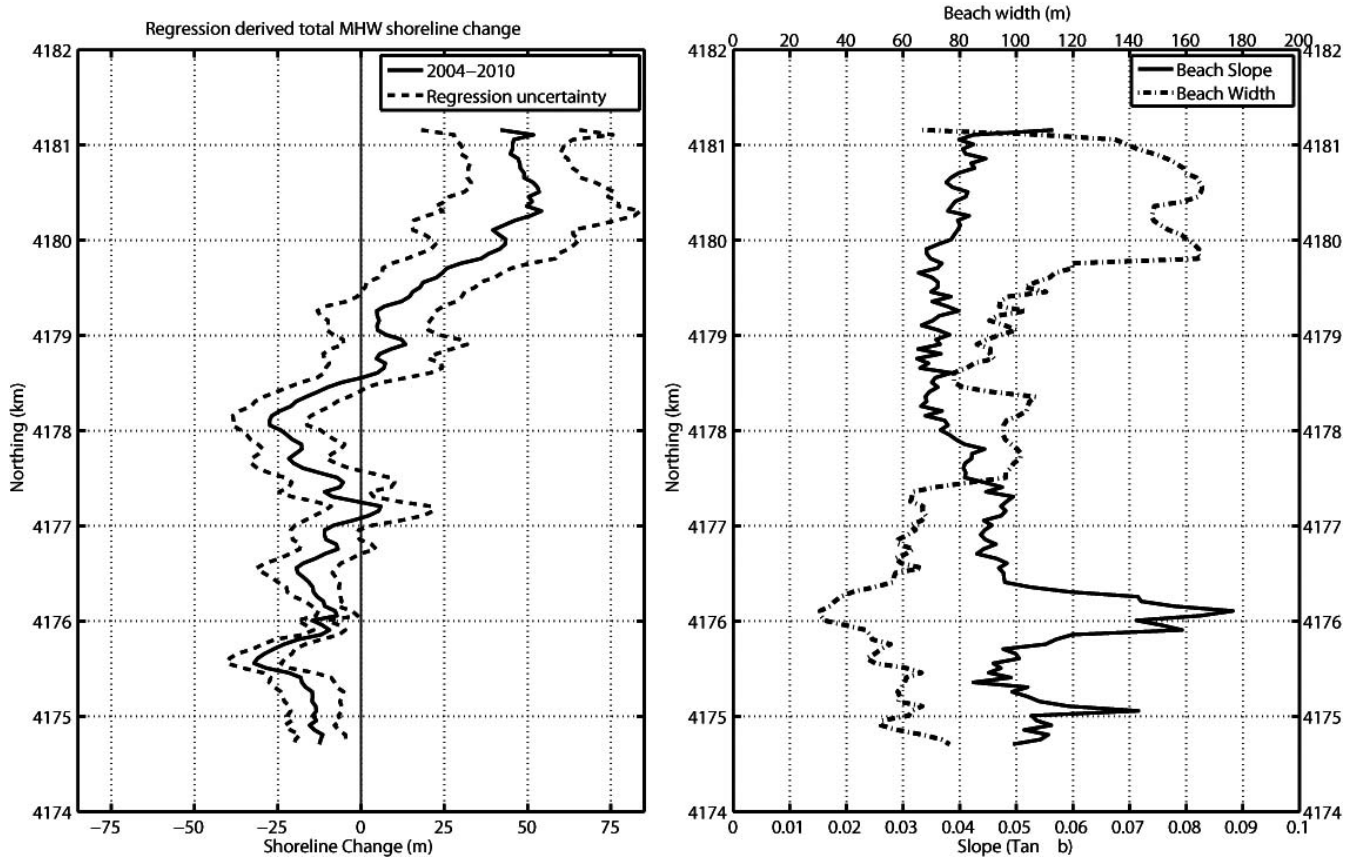

Figure 5. Alongshore variations in recent shoreline change (left), and foreshore slope and beach width (right). The erosion hot spot is centered at Northing 4176 km and is approximately 1 km in length.

instruments deployed along the approximately 11-m depth contour over a 1.2-km alongshore stretch, and six inshore surf-zone stations with buried pressure sensors and acoustic Doppler velocimeters (ADVs) or ADCPs mounted on poles within the water column. The goal of OBEX was to make observations of the hypothesized alongshore variability in wave height and wave setup along the attachment point of the southern lobe of the ebb-tidal delta. See Barnard *et al.* (2007a) and Jones (2011) for more details on these experiments.

Numerical Modeling

Three numerical modeling approaches were applied to investigate the potential causes of erosion at Ocean Beach:

(1) Simulating wave nearshore (SWAN) wave modeling (Booij, Ris, and Holthuijsen, 1999; Holthuijsen, Booij, and Ris, 1993; Ris, Holthuijsen, and Booij, 1999) was utilized to investigate the alongshore variation in wave energy at Ocean Beach (Eshleman *et al.,* 2007), as well as the change in nearshore wave energy due to multidecadal changes in ebb-tidal delta bathymetry (Dallas and Barnard, 2009, 2011).

(2) Delft3D hydrodynamic and sediment transport modeling (Lesser *et al.,* 2004) was coupled with the nearshore wave model SWAN to investigate the alongshore momentum balance and sediment transport gradients along Ocean Beach (Hansen *et al.,* unpublished data), with particular focus on the influences of the bathymetry of the San Francisco bar and sewage outfall pipe on the processes causing the erosion hot spot (Hansen *et al.,* 2011).

(3) The nearshore community model (NearCoM; Shi *et al.,* 2005) was coupled with SWAN and the quasi–three-dimensional nearshore circulation model SHORECIRC (Shi *et al.,* 2003; Svendsen, Haas, and Zhao, 2000) to investigate wave focusing along Ocean Beach (Shi *et al.,* 2011).

Historical Shoreline and Bathymetric Changes

Long-term (1850s or 1890s–2002) and short-term (1960s or 1980s–2002) shoreline change was evaluated from just east of the Golden Gate Bridge to Point San Pedro (~30 km; Figure 1). Existing digital shorelines were acquired from Hapke *et al.* (2006) and the National Oceanic and Atmospheric Administration Shoreline Data Explorer (NOAA, 2009). The data are originally from topographic sheets, digital raster graphics, and light detection and ranging (LIDAR) data sets. In addition, aerial imagery (1983) and LIDAR data (1997, 1998, and 2002) were used to supplement the existing shorelines. Short-term endpoint shoreline change rates were calculated at 50-m-spaced transects comparing the 1960s or 1980s and 2002 shoreline positions. Long-term rates of shoreline change were

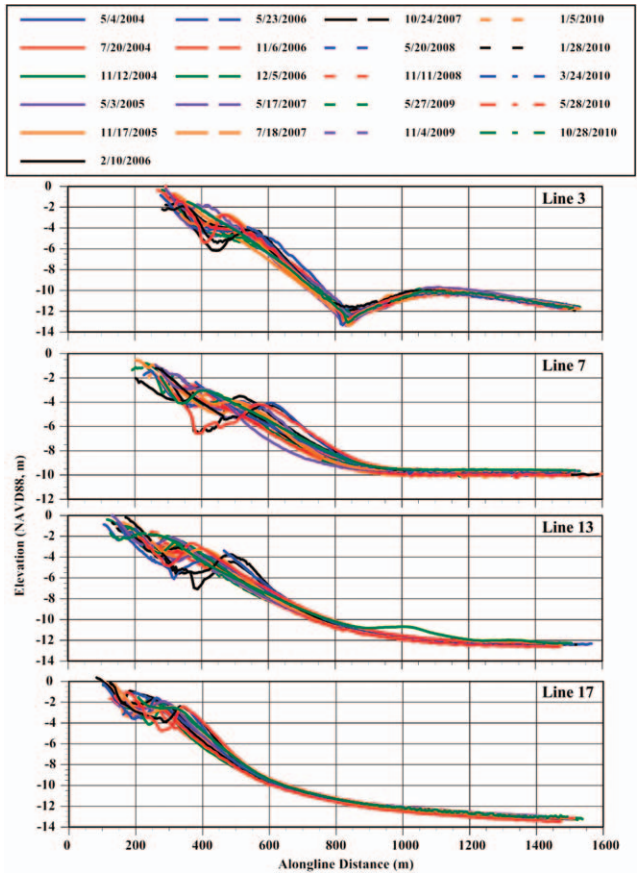

Figure 6. Variations in cross-shore morphology from CPS data lines 3 (northern end), 7 (central, on longitudinal bar), 13 (southern, hot spot), and 17 (extreme southern end) from 2004 to 2011 (see Figure 4 for transect locations).

calculated using linear regression applied to all shorelines from the earliest rates (1850s or 1890s) to 2002.

Sounding data from four historic bathymetric surveys (1873, 1900, 1956, and 2005) were used to create bathymetric grids of the San Francisco bar (Dallas and Barnard, 2009, 2011). For the 1873 and 1900 grids, soundings were digitized from hydrographic sheets obtained from the National Ocean Service (NOS). Sounding data were then registered to a common horizontal datum using the intersection of latitude and longitudinal lines (*i.e.,* graticules). For the 1956 and 2005 surveys, registered soundings were obtained directly from the NOS and from the California State University, Monterey Bay Sea Floor Mapping Lab, respectively. Bathymetric grids with a horizontal resolution of 25 m were generated for each survey. Grids were adjusted to a common vertical datum (NAVD88) to account for changes in sea-level rise (*i.e.,* tidal epoch and tidal datum) and differenced to create bathymetric change grids.

SYNTHESIS OF LOCAL ASSESSMENTS

Beach Morphology and Recent Shoreline Change

The topographic surveys at Ocean Beach between 2004 and 2010 document substantial spatial and temporal variability in

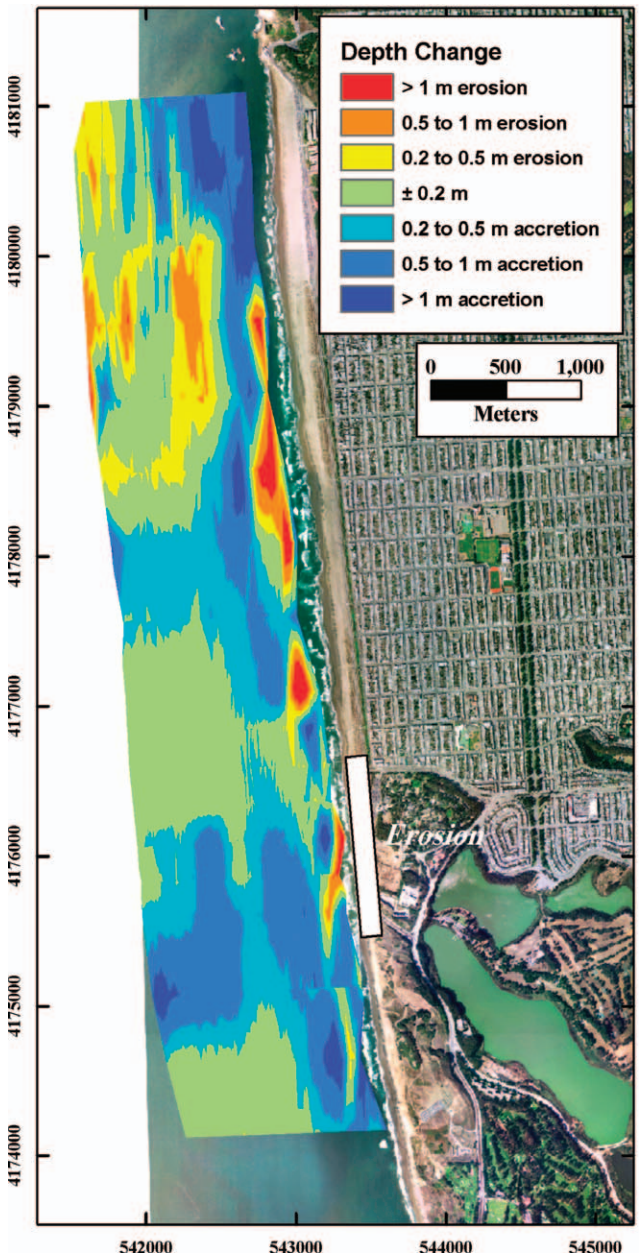

Figure 7. Nearshore bathymetric change from November 2004 to October 2010. The coordinate system is eastings (x) and northings (y) in the Universal Transverse Mercator (UTM) projection.

the subaerial beach morphology (Figure 5). In addition to seasonal changes that can amount to nearly 100 m of MHW shoreline change associated with seasonal variability in wave height, the shoreline at Ocean Beach exhibited a strong pattern of counterclockwise rotation during the study period, with the north end of the beach accreting while the south eroded (Figure 3, bottom; Hansen and Barnard, 2010). Empirical orthogonal function (EOF) analysis indicates that seasonal shoreline change is the dominant signal in the shoreline position data set, accounting for about 56% of the total

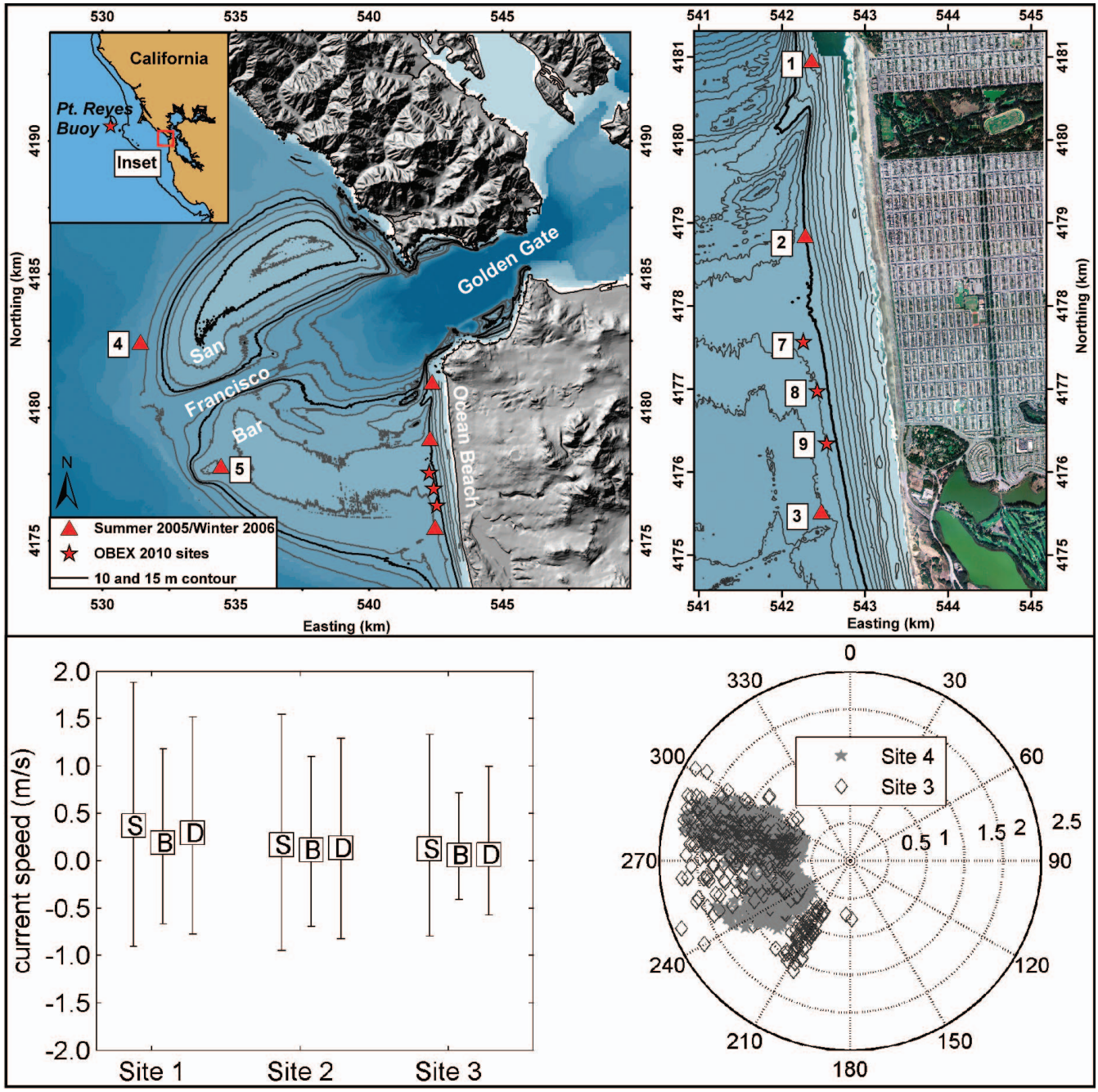

Figure 8. Top: Locations of summer 2005 and winter 2010 (OBEX) deployments. The 10- and 15-m contours are shown in black (2-m intervals to 20 m on the left panel, 1-m intervals on the right panel). Bottom: Mean, max, and minimum surface (S), bottom (B), and depth-averaged (D) alongshore currents measured during summer 2005 (lower left). The polar plot of wave direction and height for the summer 2005 deployment at sites 4 and 3 is given at the lower right.

variance. The second EOF mode, accounting for about 16% of the variance, is the rotational signal in the shoreline. For Ocean Beach, the rotational signal accounts for an increasing percentage of the variance as the temporal span of the shoreline record length increases.

Beach width and foreshore slope along Ocean Beach also vary considerably (Figure 5, right). At the north end of the beach, the mean beach width exceeds 160 m in some areas, while in the more erosional area in the south, the mean beach width is only about 30 m. The MHW shoreline eroded as much as 32 m in the erosion hot-spot area between 2004 and 2010 (Figures 3, bottom, and 5). Additional landward erosion in the hot-spot area is limited due to armoring (*e.g.,* Figures 5, Northing 4176, and 3, bottom). The impact of the armoring is particularly evident in the foreshore slope at Northing 4176 km (Figure 5).

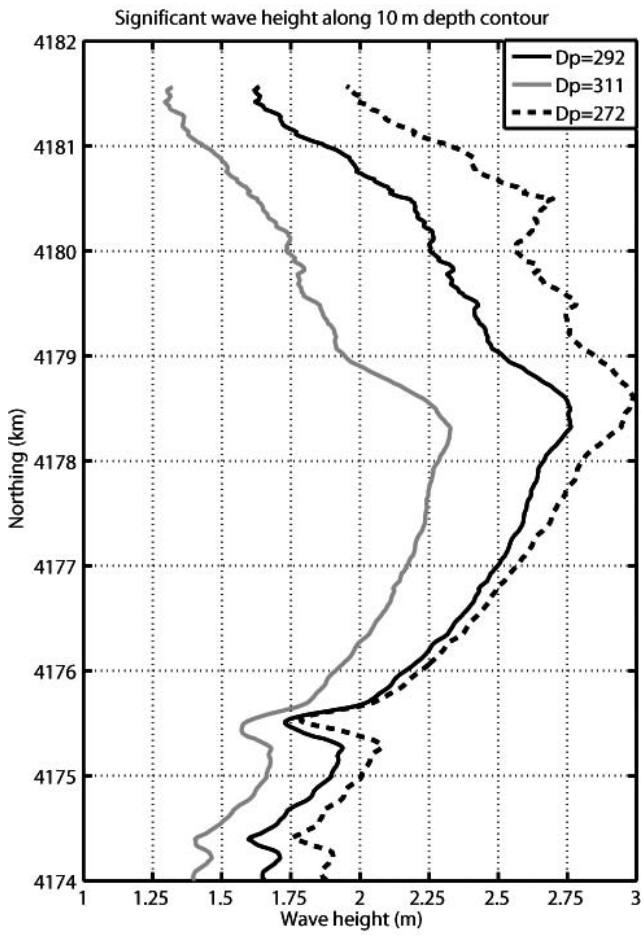

Figure 9. SWAN predicted alongshore variations in wave height at the 10-m contour at Ocean Beach from three wave cases. The model was forced with 2.5-m offshore significant wave height and 14-s peak period but with differing directions of 272°, 292°, and 311°.

Nearshore Morphology and Recent Bathymetric Change

The shape of the nearshore profile and the intra-annual variability is controlled to varying degrees by both wave exposure and location within the ebb-tidal delta complex along Ocean Beach (Figure 6). The flattest profiles with the greatest intra-annual variability occur in the center (*e.g.,* Figure 6, line 7), where the longitudinal bar attaches to the beach and the largest waves are found (Figure 1). Conversely, the steepest and least variable profiles are located at the extreme southern end of the beach (*e.g.,* Figure 6, line 17), in the shadow of the ebb-tidal delta. The profiles in the erosion hot-spot region (*e.g.,* Figure 6, line 13) are intermediate between the central portion and the extreme southern end of the beach, with moderate slopes and intra-annual variability. Profiles at the northern end of the beach (*e.g.,* Figure 6, line 3) are subjected to strong tidal influence, with a large tidal channel cutting directly through the nearshore region, but also exhibit evidence of strong alongshore transport during extreme events (Barnard, Hoover, and Hansen, 2011). Bathymetric change from the CPS surveys between November 12, 2004, and October 28, 2010, is shown in Figure 7. The bathymetric survey region experienced mean vertical accretion of 0.22 m, which equates to a total volume change of +1.95 million m^3. A significant amount of this accretion can be attributed to the extreme net nearshore accretion observed during the recent El Niño year (May 2009–May 2010), a total of 1.6 million m^3 of sediment (Barnard, Hoover, and Hansen, 2011). However, the spatial patterns of bathymetric change are consistent with the observed shoreline trends from 2004 to 2010 (Figure 5) and from 2004 to 2009 (Hansen and Barnard, 2010). For example, at the northern end of the beach, high rates of shoreline accretion correlate with high rates of nearshore accretion, indicative of the overall counterclockwise rotation of both the beach and the nearshore regions. Erosion generally dominates the extreme nearshore (*i.e.,* depths of ~5 m) in the central portion of the beach, while a narrow but prominent pocket of erosion is located immediately adjacent to the erosion hot spot. Significant amounts of accretion are present offshore and to the south of the longitudinal bar and the erosion hot spot, the latter being influenced by annual nearshore dredge disposal placement from 2005 to 2010 (Barnard, Erikson, and Hansen, 2009; Barnard *et al.,* 2009). Overall, the observed bathymetric change from 2004 to 2010 is indicative of sediment loss from the beach and gain to the extreme northern part of the beach and offshore.

Alongshore Variability in Physical Forcing

Currents and Waves

In summer 2005, three ADCPs were deployed in the nearshore at Ocean Beach, and an additional instrument was placed on the NW edge of the ebb-tidal delta (Figures 4 and 8). Sites 1 (north end) and 2 (north–central) were north of the longitudinal bar, and site 3 (south end) was just offshore of the erosion hot-spot region. The northern section of the beach experienced strong alongshore currents, peaking at nearly 2 m/s at the surface during the flooding stage (mean depth average 0.4 m/s), whereas the north–central and southern stretches had mean current magnitudes that were less than half as strong (Figure 8). However, this relationship holds only on the flooding tide. On the ebbing tide, current speeds at the south end (site 3) can equal or exceed those measured in the northern section of the beach, likely due to the ebb being dominated by a jet that extends straight west of the inlet, thereby limiting the currents along Ocean Beach (Barnard *et al.,* 2007a). These currents flowed along the coast, were dominated by tidal forcing, and had a very small landward component of flow. The strongest currents were at the surface, and vertical gradients in current magnitude showed velocities varying by as much as 1 m/s throughout the water column, with an average vertical range of velocities on the order of 0.25 m/s (Figure 8).

While the northern portion of the beach experienced stronger currents overall, wave energy was much greater in the southern portion near the erosion hot spot. This is reflected in the higher measurements of significant wave height at site 3 compared to sites 1 and 2 (Barnard *et al.,* 2007a). Site 4 had higher angles of incidence by approximately 30° than directions

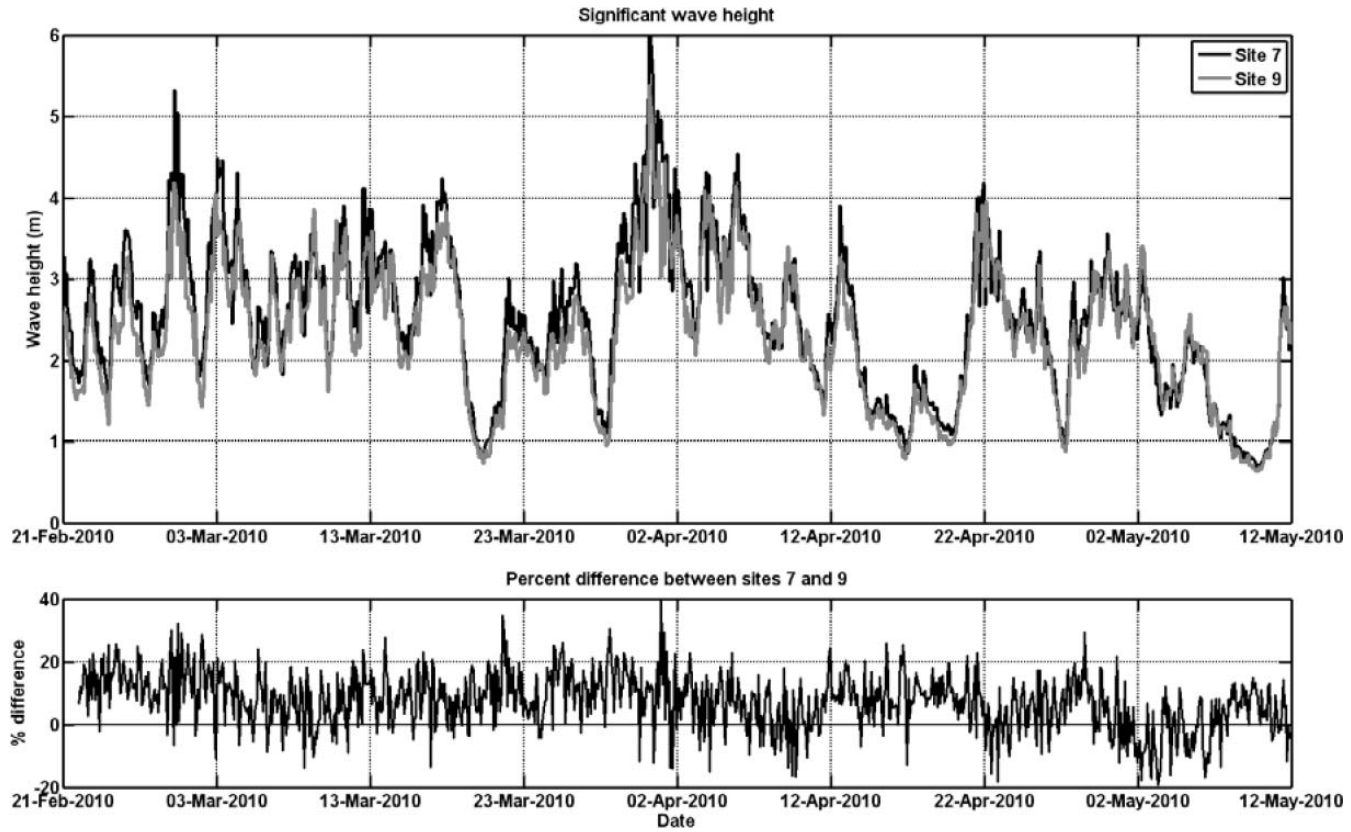

Figure 10. Comparison of significant wave heights measured at sites 7 and 9 (see Figure 8, top, for instrument locations). The red curve is the significant wave height measured at site 9; the black curve is the significant wave height at site 7. The black curve in bottom panel shows the percent difference between wave heights at the two sites.

measured at the inshore sites due to refraction across the ebb-tidal delta (Figure 8).

The spatial variability in wave conditions along Ocean Beach due to refraction across the ebb-tidal delta was investigated using the SWAN wave model. Tide-cycle (24.8 h), averaged, predicted significant wave heights from a coupled SWAN–Delft3D model of three common offshore wave cases, all with an offshore significant wave height of 2.5 m and a period of 14 s but with the differing directions of 272°, 292°, and 311°, are shown in Figure 9. Waves that approach the coast from the W (~270°) and W–NW (~290°) are strongly focused by the ebb-tidal delta, resulting in considerable alongshore variability in wave height along Ocean Beach. The largest waves occur around Northing 4178 to 4179 km, where the longitudinal bar merges with the shoreline in the middle of Ocean Beach. Wave focusing by the ebb-tidal delta can result in a more than 70% increase in wave energy from the south end of Ocean Beach to the wave focal zone. Waves that approach the coast from the NW (~315°) are less focused and more dissipated by the ebb-tidal delta prior to reaching Ocean Beach, and they do not exhibit as much alongshore variability in wave energy (Figure 9).

Field measurements obtained during the OBEX experiment (Figure 8) confirm these findings. During the 4-month-long deployment, offshore significant wave heights up to 6 m were recorded. The most northerly instrument at site 7, closest to the apex of the longitudinal bar, consistently recorded wave heights larger than the sites to the south, with as much as a 40% greater wave height between sites 7 and 9 (mean difference 0.18 m; Figure 10). Correspondingly, the inshore, surf-zone pressure sensors recorded a similar pattern of wave-induced setup during the 2-week deployment, with water levels about 10 cm higher in the north, compared to 600 m farther to the south (Hansen *et al.,* unpublished data; Jones, 2011). The alongshore variation in wave height and the corresponding wave-induced setup result in significant pressure gradients that sometimes dominate nearshore circulation patterns. Even during moderate conditions at Ocean Beach (deep-water significant wave height [H_s] = 3.5 m, peak wave period [T_p]= 15 s, and peak wave direction [D_p] = 270°), NearCoM results indicate that setup can vary by 30 cm alongshore—0.4 m in the center of the beach near the wave focal point, 0.1 m in the extreme south (Shi *et al.,* 2011). Alongshore variability of forcing in the surf zone has direct implications on the persistence of the hot spot, leading to gradients in the velocity field and thus transport of sediment.

Nearshore Hydrodynamics and Effects of the Exposed Outfall Pipe (Delft3D)

A 200-m-wide trough in about 12- to 16-m water depth is associated with the scour of an exposed rock crown covering an outfall pipe offshore of the erosion hot spot (Figures 1 and 11).

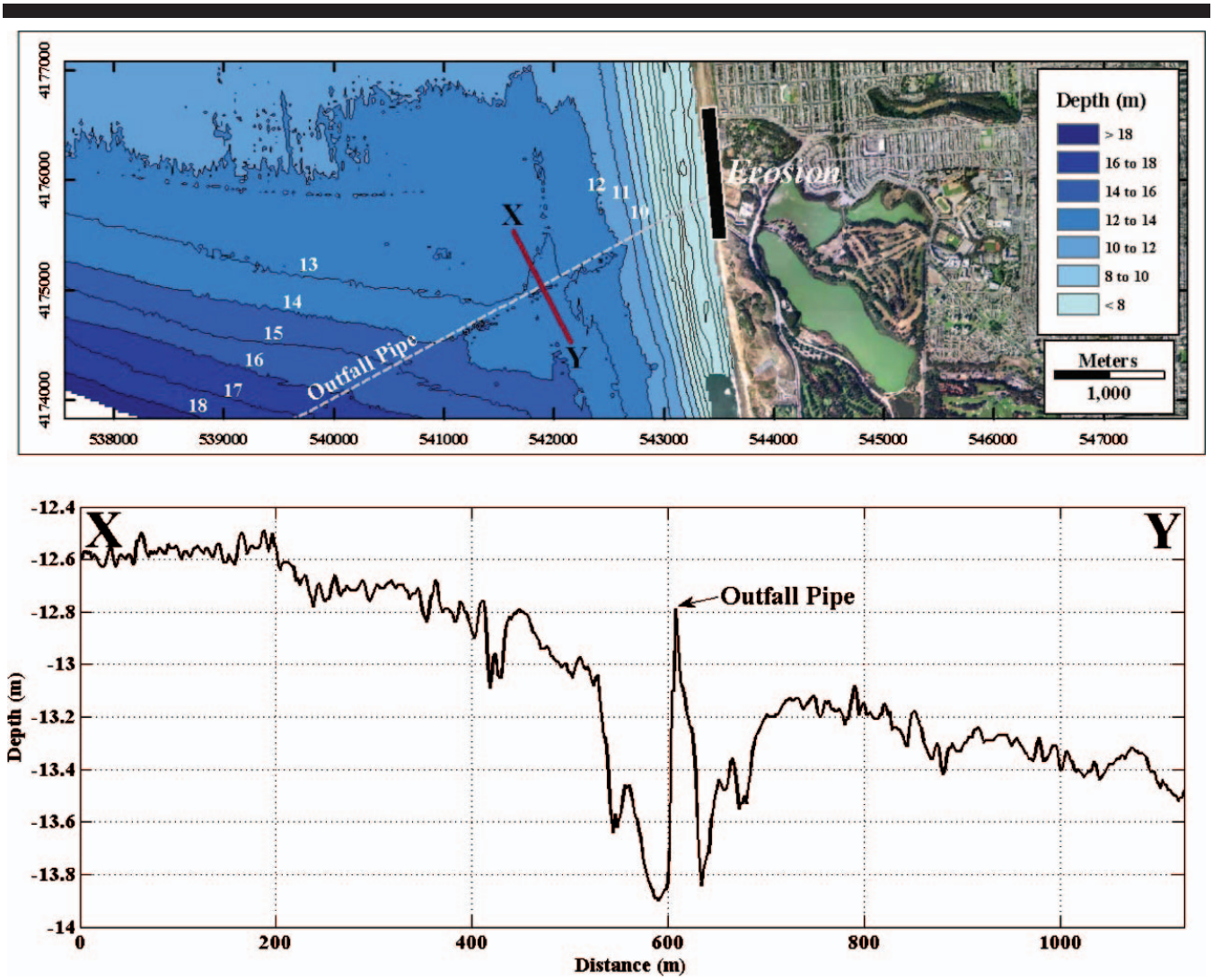

Figure 11. Detail of the bathymetry at the southern end of Ocean Beach (top) with the cross-section across the outfall pipe from the May 2005 multibeam survey (bottom). The coordinate system is eastings (x) and northings (y) in the UTM projection.

The scour was observed during a multibeam bathymetry survey of the entire mouth of San Francisco Bay in 2004–05 and subsequently confirmed by more than a dozen surveys exclusively in the outfall pipe vicinity from 2005 to 2010 (Barnard, Erikson, and Hansen, 2009; Barnard *et al.,* 2007a, 2007b, 2009).

Delft3D was used to analyze the alongshore momentum balances for the entire extent of Ocean Beach (Hansen *et al.,* unpublished data) with particular emphasis on exploring the influence of the ebb-tidal delta and the outfall pipe on the basic forcing terms (*i.e.,* radiation stress and pressure gradients; Hansen *et al.,* 2011). The model predicted flow patterns that were favorable for sediment removal from the erosion hot-spot area and net erosion from the surf zone. Analysis of the forcing terms driving surf-zone flows revealed that wave refraction over the exposed wastewater outfall pipe between the 12- and the 16-m isobaths introduces a perturbation in the wave field that results in erosion-causing flows (Figure 12). The model predicts that the scour adjacent to the outfall leads to upward of a 0.5-m decrease in local wave heights over the pipe, refracting waves away from the trough much like a submarine canyon, albeit on a much smaller scale. Although the scour does not extend inshore of an approximately 12-m depth, modifications to the wave field still exist in the surf zone and lead to a large discontinuity in both pressure and radiation stress gradients. These perturbations in the flow-forcing terms together cause a persistent rip current and alongshore flow acceleration (Figure 12). These flows appear under a variety of wave and tidal conditions but are most apparent when offshore waves approach the coast from the prevalent W to W–NW directions (~270°–300°). Modeled potential alongshore sediment transport gradients indicate sediment removal from the erosion hot-spot area (Figure 12).

SYNTHESIS OF REGIONAL ASSESSMENTS

After focusing on the morphodynamics directly impacting the erosion hot spot at Ocean Beach due to the outfall pipe and the shape of the ebb-tidal delta, it is important to describe this small

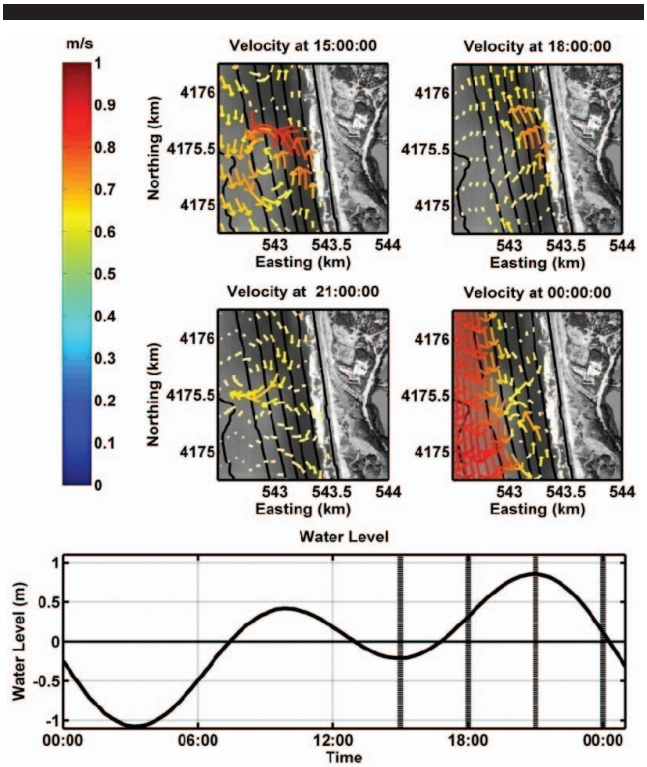

Figure 12. Map view of the flow patterns at four tidal stages offshore of the erosion hot spot and onshore of the wastewater outfall pipe, showing the persistent rip current that develops as a result of the perturbation in the wave field caused by scour surrounding the pipe. The vertical bars in the lower panel indicate the tidal stage of the four output times shown (Hansen *et al.,* 2011).

area in the context of the evolution of the entire coastal system. The Golden Gate inlet is the sole connection linking the open coast (*i.e.,* the ebb-tidal delta and adjacent beaches) with the San Francisco Bay estuary, collectively referred to as the San Francisco Bay coastal system. The Golden Gate provides the conduit for the daily transport of about 8 trillion L of water (8×10^9 m^3, 93,000 m^3/s), which carries mud, sand, biogenic material, nutrients, and pollutants in and out on the tides. Therefore, any significant changes to San Francisco Bay and the 29 watersheds that drain into it, particularly modifications to the tidal prism, sediment supply, or freshwater discharge, can significantly influence coastal processes at the mouth of San Francisco Bay, including the ebb-tidal delta and adjacent open-coast beaches.

Historical Changes to the San Francisco Bay Coastal System

The San Francisco Bay coastal system has been significantly impacted by anthropogenic activities since the mid-19th century (Figure 13). Hydraulic mining during the Gold Rush released about 850 million m^3 of sediment into San Francisco Bay watersheds in the second half of the 19th century (Gilbert, 1917). Bay development, including the filling or diking of 95% of the tidal marsh areas from 1850 to the late 20th century, reduced the tidal exchange surface area by about two-thirds (Atwater *et al.* 1979) and tidal prism by about 10% (Conomos, 1979; Dallas and Barnard, 2011; Gilbert, 1917; Keller, 2009). Over the last century, a minimum of 200 million m^3 of sediment has been permanently removed from the San Francisco Bay coastal system through dredging, aggregate mining, and borrow pit mining, including at least 54 million m^3 of sand-sized or coarser sediment from central San Francisco Bay, immediately adjacent to the Golden Gate inlet (Dallas and Barnard, 2011). In addition, Wright and Schoellhamer (2004) demonstrated that modifications to the Sacramento and San Joaquin River deltas, the primary watersheds feeding San Francisco Bay, have resulted in an approximately 50% reduction in suspended sediment flux to the bay from 1957 to 2001. The waning of the hydraulic mining signal by the mid-20th century (Porterfield, 1980), coupled with delta modifications and direct removal of sediment from the bay floor, is reflected in the volumetric seabed change that has been recorded from San Francisco Bay (Capiella *et al.,* 1999; Fregoso, Foxgrover, and Jaffe, 2008; Jaffe, Smith, and Torresan, 1998) and the ebb-tidal delta (Dallas and Barnard, 2011; Hanes and Barnard, 2007) over the last 50 years: a total of about 240 million m^3 of sediment loss, including 14 million m^3 of predominantly coarse sediment loss in just the last decade from west–central San Francisco Bay, linked primarily to aggregate mining (Barnard and Kvitek, 2010).

Very large, ebb-dominated bedforms were mapped during the 2004–05 multibeam survey in the inlet throat (Barnard *et al.,* 2006), and an extensive study of bedform asymmetry (a proxy for bedload transport) throughout the mouth of San Francisco Bay and the west–central San Francisco Bay (Barnard *et al.,* 2012) indicates that net *potential* sand transport along the seabed is ebb directed (Figure 14, top). In addition, boat-mounted, cross-channel ADCP transect-calculated discharge and sediment flux across the inlet throat clearly supports the hypothesis that tidal sand transport *potential* is ebb dominated. This finding was confirmed by a numerical modeling exercise in which the annual sand transport volumes were estimated based on a 36-day hydrodynamic tidal simulation (no wave modeling) that is a proxy for annual behavior (Barnard *et al.,* 2012, Figure 14, bottom). Therefore, if sediment availability in San Francisco Bay becomes progressively limited, less sediment will be transported seaward to the ebb-tidal delta and open-coast beaches. Given the many factors that have limited sediment availability in San Francisco Bay over the last century (*e.g.,* decay of the hydraulic mining signal, damming and diversion of sediment in the San Joaquin River and Sacramento River deltas, widespread development of wetlands, borrow pit mining, dredging, and aggregate mining), in addition to the continued removal of coarse sediment by aggregate mining at a rate of about 1 million m^3/y, there is every indication that this trend of sediment loss will continue. Furthermore, with projections of sea level rise (*e.g.,* Vermeer and Rahmstorf, 2009) likely to increase the depth of San Francisco Bay over the coming decades, the estuary would become a more efficient sediment sink, though localized scour potential may increase due to the enlarged tidal prism. Nevertheless, these factors generally indicate that the potential rate of coarse sediment transport from the bay to the ocean will certainly not accelerate over recent rates and will probably continue to decline for the foreseeable future.

Figure 13. Overview of historical changes to the San Francisco Bay coastal system. See the text for references to reported bathymetric change and anthropogenic influences.

Ebb-Tidal Delta Evolution

Similar to most regions inside San Francisco Bay, from 1956 to 2005, the mouth of San Francisco Bay lost sediment (−92 million m³; Hanes and Barnard, 2007), in particular the ebb-tidal delta (−76 million m³; Dallas and Barnard, 2011; Figure 15). The pattern of change can be characterized by ebb-tidal delta contraction whereby the outer lobe eroded heavily, with some accretion on the interior. A radial pattern of contraction has been prevalent during the other survey intervals as well (*i.e.,* 1873–1900 and 1900–56), even during an episode of volumetric accretion. Because there has been no significant change in the wave climate to cause contraction, the period of accretion (1900–56) is linked to an increase in sediment supply, coupled with a reduction in tidal prism (Dallas and Barnard, 2011). During the last half of the 20th century, minimal infilling of the bay occurred, so the pervasive erosion and contraction of the ebb-tidal delta from 1956 to 2005 is attributed primarily to a reduction in sediment supply to the mouth of San Francisco Bay.

The pattern of ebb-tidal delta contraction has direct implications on the southern end of Ocean Beach in the vicinity of the erosion hot spot. The southern outer lobe of the ebb-tidal delta that formerly provided protection to southern Ocean Beach from direct wave attack in 1956 migrated about 1 km to the north by 2005, leaving the seabed about 1 to 2 m deeper offshore of the present erosion hot spot (Figure 15, inset). Using SWAN, Dallas and Barnard (2011) showed that the change in bar bathymetry from 1956 to 2005 resulted in an approximately 10% increase in wave power in the erosion hot-spot region during typical winter storms. The greater depth reduces nearshore wave energy dissipation; therefore, larger waves can directly impact this section of coastline. In addition, wave-induced onshore sediment transport that has been hypothesized to occur along the crest of the ebb-tidal delta toward Ocean Beach (Battalio and Trivedi, 1996) no longer has the potential to directly feed this region.

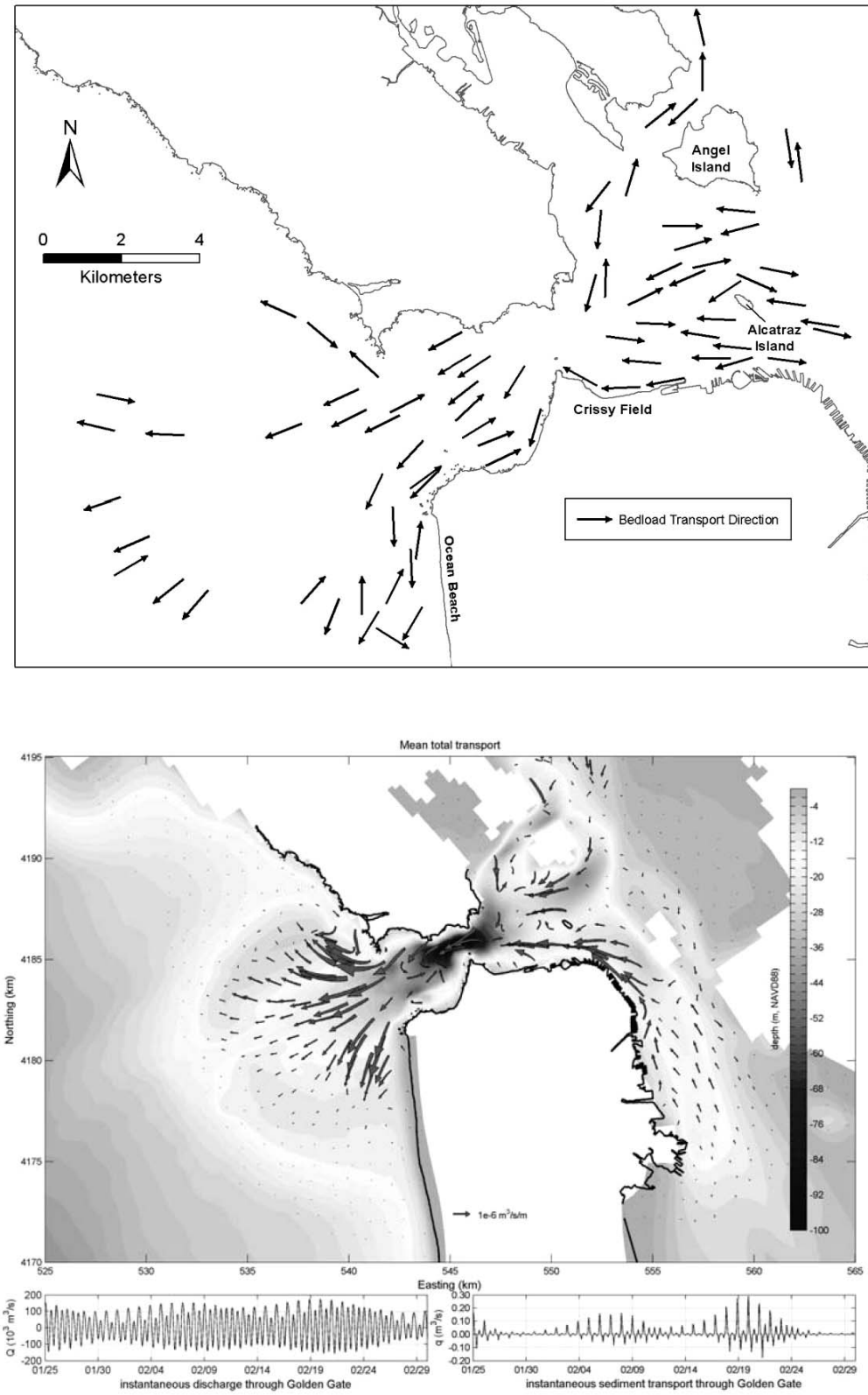

Figure 14. Evidence for potential ebb-directed sediment transport. Top: Bedform asymmetry indicating ebb-dominated transport through the Golden Gate. Bottom: Delft3D-modeled residual tidal transport, also indicating ebb dominance (both plates modified from Barnard *et al.,* 2012).

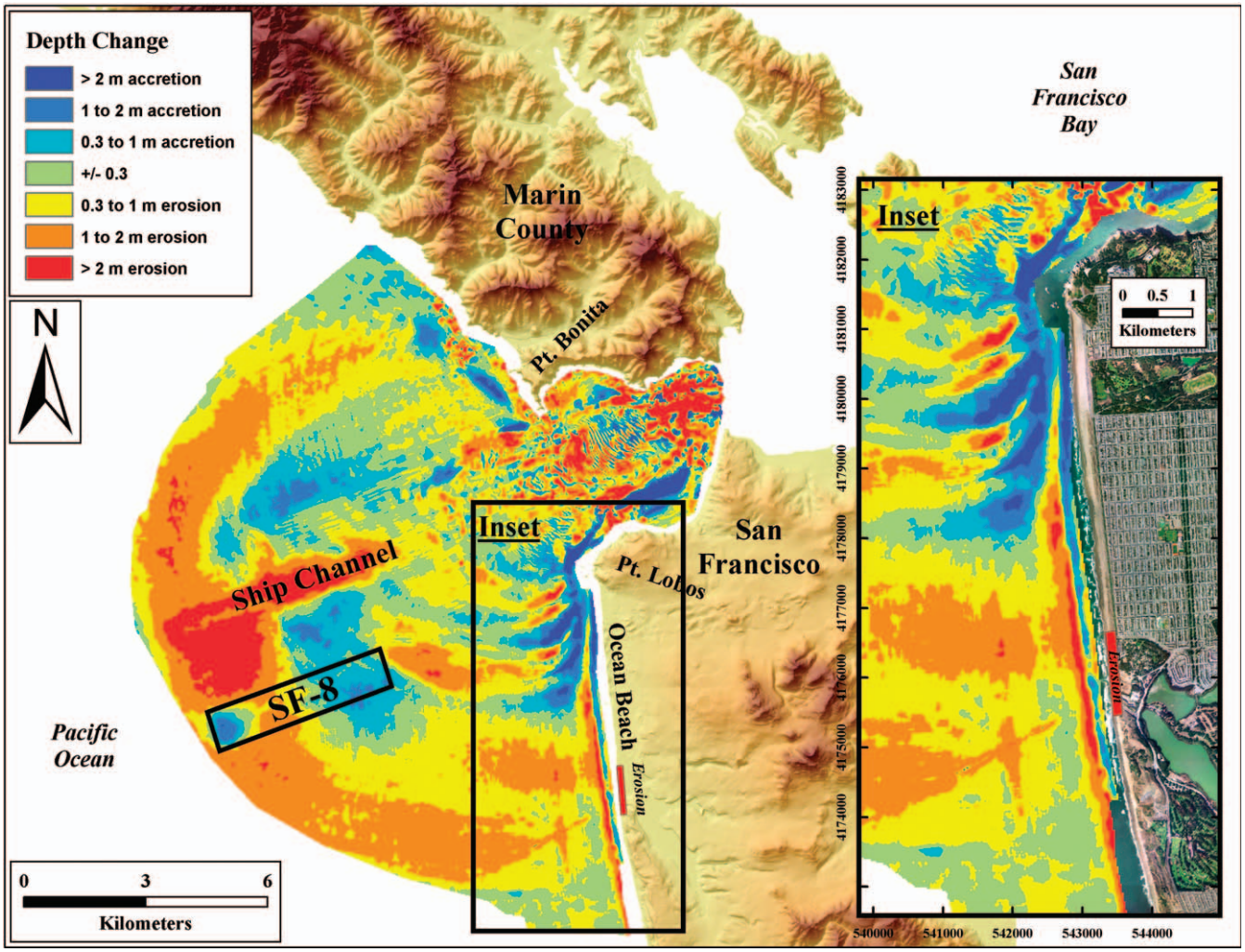

Figure 15. Bathymetric change at the mouth of San Francisco Bay from 1956 to 2005. In the inset, the coordinate system is eastings (x) and northings (y) in the UTM projection.

Regional Shoreline Changes

The radial contraction and erosion of the ebb-tidal delta and systemwide sediment loss are also reflected in the short- and long-term trends of shoreline change along the outer coast adjacent to the mouth of San Francisco Bay (Figure 16). Shoreline change rates were calculated for long-term (1850s–90s to 2002) and short-term (1960s–80s to 2002) periods.

In the shadow of the ebb-tidal delta along the San Francisco shoreline, from Crissy Field to northern Ocean Beach, the majority of the coastline was accreting in the long term (86%) and short term (87%), with the rate of accretion accelerating threefold to +0.6 ± 0.4 m/y. Accretion also dominated the northern half of Ocean Beach during both periods, suggesting more sediment is available for northerly transport, possibly due to flood channel infilling and ebb-tidal delta contraction, both of which could result in an increase in sediment supply to this area.

However, from the middle of Ocean Beach south to the end of the littoral cell at Point San Pedro, erosion dominates the shoreline change signal. Nearly the entire coast south of the ebb-tidal delta (San Mateo) was heavily eroding in the long term (93% of all transects) and short term (98% of all transects), with the rate increasing by 50% (−0.6 ± 0.3 m/y) in the last several decades. In addition, shoreline change results for the state of California by Hapke *et al.* (2006) showed that the stretch of coastline from Point Lobos (*i.e.,* the northern boundary of Ocean Beach) to Davenport (~80 km south of Point San Pedro), which includes the Ocean Beach and San Mateo regions covered in this study, has the highest regionally averaged long-term erosion rate in the state. Together, these results indicate widespread erosion along the outer coast adjacent to the mouth of San Francisco Bay, with an increase in erosion rates in recent decades. The area south of Ocean Beach has always been beyond the direct influence of significant tidal current sediment transport from San Francisco Bay, so the likely cause of the erosional trend is a reduction in the sediment supply to the region. Eustatic sea level rise has been suppressed along the U.S. West Coast since

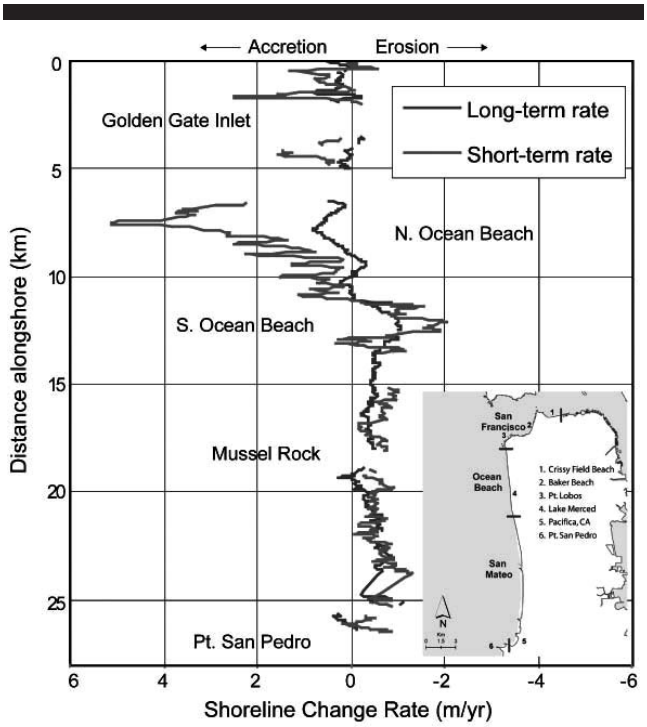

Figure 16. Regional historical shoreline changes. Distance is from the San Francisco Marina inside the estuary (modified from Dallas and Barnard, 2011).

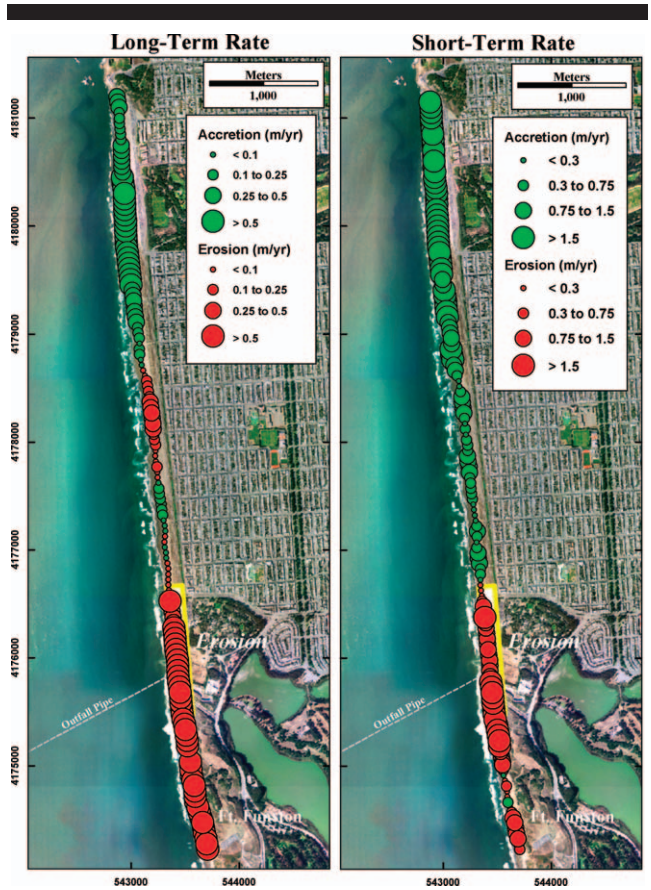

Figure 17. Historical shorelines changes along Ocean Beach. The long-term rate (linear regression) is from 1899 to 2002, and the short-term rate (end point) is from 1983 to 2002. The coordinate system is eastings (x) and northings (y) in the UTM projection.

1980 (Bromirski *et al.,* 2011) and therefore is ruled out as a factor in any recent shoreline changes. The transition from trends of accretion to trends of erosion at Ocean Beach occurs where the crest of the ebb-tidal delta attaches to the shoreline (Figure 17). Therefore, it appears that the shape of the ebb-tidal delta, in particular the location of the crest, exerts dominant control on shoreline change at Ocean Beach. Dallas and Barnard (2011) showed that in the central and southern sections of Ocean Beach, shoreline change and significant wave height change at the 10-m contour are well correlated for winter storm conditions from the 1950s to the 2000s, with an increase in nearshore wave height linked to shoreline erosion and the highest correlation in the vicinity of the erosion hot spot. Given that some climate models suggest an increase in El Niño–like conditions in California over the coming decades, possibly resulting in more frequent and intense storms (*e.g.,* Cayan *et al.,* 2008), as well as recent trends of increasing wave heights (especially extreme waves) for much of the California coast (Allan and Komar, 2006; Wingfield and Storlazzi, 2007), there is every indication that increasingly powerful waves will impact the exposed southern portion of Ocean Beach.

Decadal Grain Size Variations

At the mouth of San Francisco Bay, mean grain size generally correlates with tidal velocity magnitude, fining from coarse sand and gravel in the inlet throat (*i.e.,* the Golden Gate) to very fine sand on the outer reaches of the ebb-tidal delta and inner continental shelf (Figure 18). As the delta contracts, as a result of decreasing sediment supply, weaker tidal currents due to tidal prism reduction, or both, the outer reaches should become progressively finer. This could be a result of either finer shelf sediment being exposed or transported shoreward by wave action or finer sediment coming out of the bay. Regardless, annual sediment sampling from up to 56 stations between 1997 and 2008 shows a fining of mean grain size by about 25 μm (Figure 18b). This fining is also reflected in the percent mud (Figure 18c) and percent sand (Figure 18d) content of the samples. Between 2002 and 2007, there was a substantial shift to progressively finer sediment along the outer reaches of the ebb-tidal delta. Of particular note is the pervasive fining to the north and south of the ebb-tidal delta and the much finer sediment immediately offshore of the erosion hot spot. Finer, more easily erodible sediment offshore of southern Ocean Beach could be an additional contributing factor to the vulnerability of the site. The regional-scale fining of sediment at the mouth of San Francisco Bay from 1997 to 2008 may be related to the observed 36% step decrease in suspended sediment concentrations (SSCs) observed inside the bay between the 1991–98 and the 1999–2007 water years, broadly attributed to the depletion of the "erodible sediment pool" that was once filled with pulses of sediment due to the effects of hydraulic mining and urbanization, and further reduced by sediment trapping behind dams (Schoellhamer,

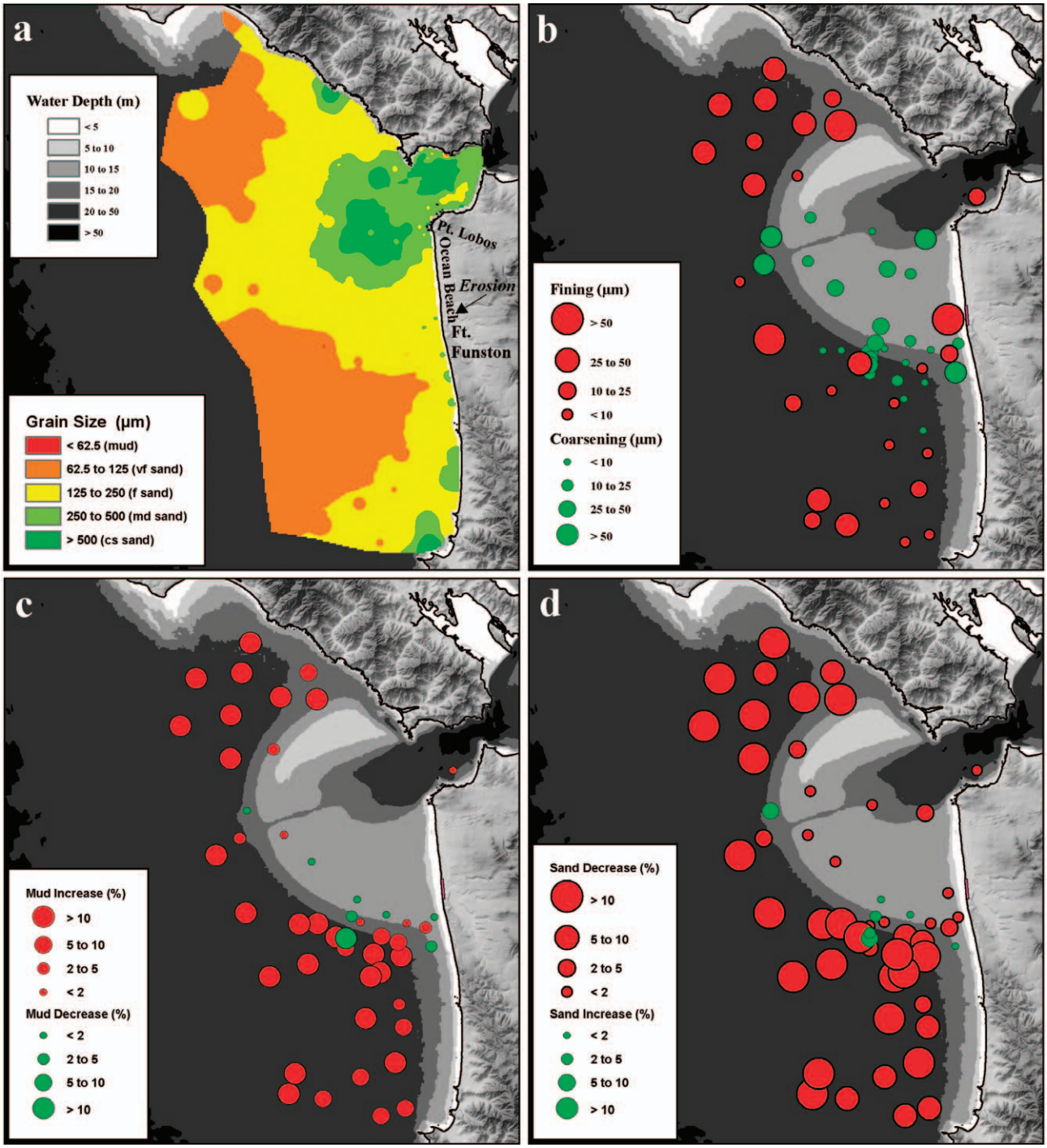

Figure 18. Grain size at the mouth of San Francisco Bay. (a) Gridded grain size from mean of samples collected from 1997 to 2008 (n = 56), and single samples collected in 2005, 2008, and 2010 (n = 385; sample sites shown in Figure 4). (b) Change in mean grain size from 1997 to 2008. (c) Change in percent mud from 1997 to 2008. (d) Change in percent sand from 1997 to 2008.

2011). The decrease in SSCs, and presumably by proxy in coarser bedload, could affect the mouth of San Francisco Bay in two primary ways. First, this flushing of erodible, mostly fine sediment could have been transported seaward through the Golden Gate inlet, settling on the distal edges of the ebb-tidal delta and vicinity and reducing the bed grain size. Second, the observed reduction of suspended sediment from 1991 to 2007 inside San Francisco Bay is indicative of a limited supply to the mouth of San Francisco Bay; therefore, fine, wave-driven shelf sediment became more prevalent or continued contraction of the

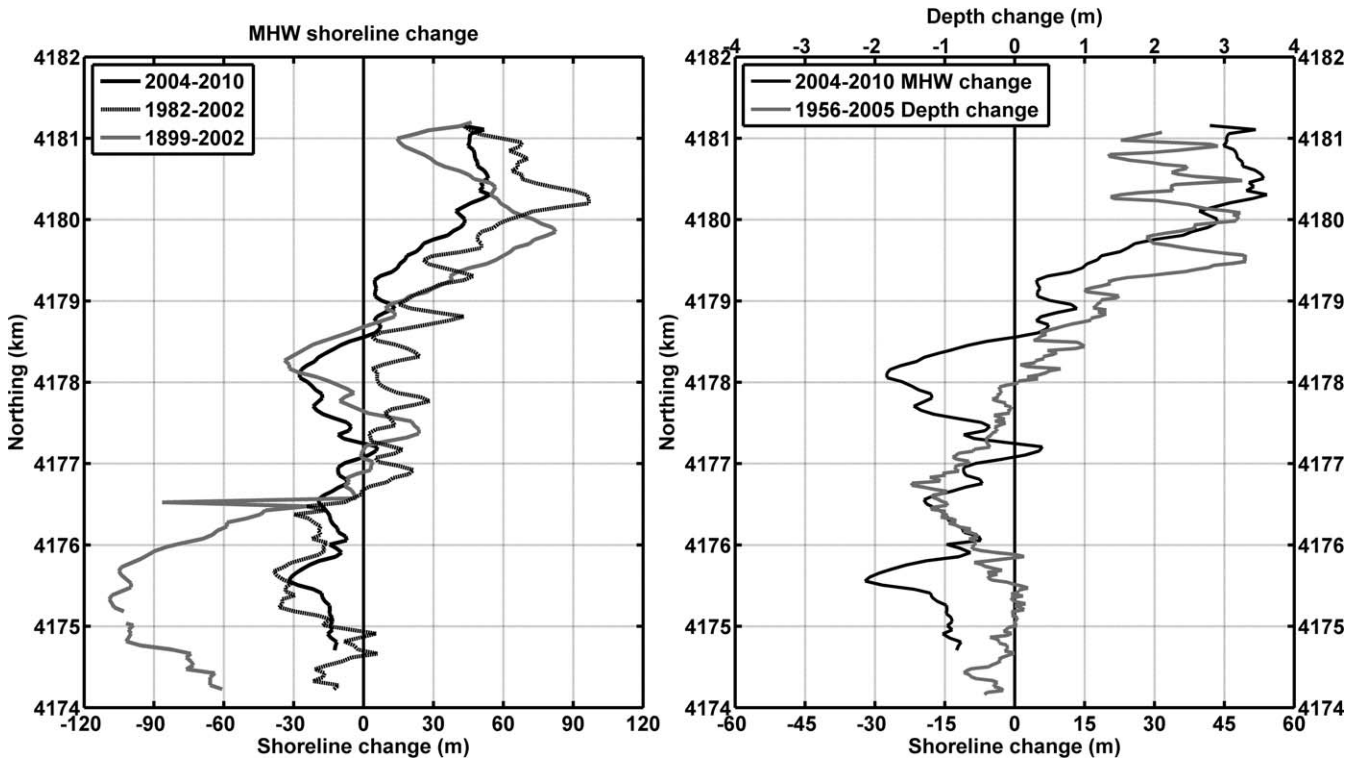

Figure 19. Left: Alongshore variations at Ocean Beach of regional historical long-term (1899–2002) and short-term (1983–2002) shoreline change rates and recent (2004–10) shoreline change rates. Right: Comparison of nearshore bathymetric change from 1956 to 2005 along the 10-m bathymetric contour (from the 2005 multibeam survey) and recent shoreline change rates.

ebb-tidal delta exposed finer sediment. Either way, progressively finer sediment, coupled with an increase in wave energy (see the previous section), will continue to favor erosion in the southern portion of Ocean Beach.

FINAL SYNTHESIS

The rotational signal in the MHW shoreline at Ocean Beach (Figures 5 and 19) directly follows the pattern seen in the ebb-tidal delta evolution (Figure 15). Transition from shoreline accretion to erosion along the beach at all temporal scales occurs at the same approximate alongshore area as the bathymetric change between 1956 and 2005 (Figure 15), which also switches from accretion to erosion (Figure 19). The patterns in the MHW shoreline change, beach width, and change in the ebb-tidal delta indicate that the delta exerts first-order control on multiannual beach change. The changes in the subaerial beach follow the historic changes observed in the ebb-tidal delta. Thus, as the delta has contracted (Figure 15) the beach in the erosion hot-spot area has narrowed following the erosion of sediment offshore of the hot-spot area.

A variety of data collection techniques and numerical modeling approaches have been integrated to explore the cause of an erosion hot spot at Ocean Beach. The collective approach describes a coastal system that is highly variable alongshore, both in morphology and in physical forcing. The shape of the ebb-tidal delta and proximity to the tidal inlet are the dominant controls on the observed variability in nearshore circulation patterns and coastal evolution. The shape of the ebb-tidal delta, in turn, has been significantly altered by a massive loss of sediment, on the order of 0.25 billion m^3, from the San Francisco Bay coastal system over the last half century. Ultimately, the shape of the ebb-tidal delta, especially the precise location of the longitudinal bar that dictates the location of intense wave focusing, determines the nearshore circulation patterns and areas prone to erosion. The entire stretch of shoreline south of the longitudinal bar experiences erosion, and points north have been accreting. If the observed trend of ebb-tidal delta contraction continues, this nodal point is likely to migrate northward, exposing more beach to critical erosion. The erosion hot spot along the 1-km section of coast south of the longitudinal bar attachment point at Ocean Beach exists for the following reasons: (1) the shoreline was artificially built out during expansion of the City of San Francisco in the early 1900s; (2) systemwide loss of sediment leads to contraction of the ebb-tidal delta, which in turn reduced sediment supply to the area; (3) southward decreasing wave heights under most conditions result in alongshore gradients in the flows and sediment transport; and (4) the scour of the outfall pipe and associated rock crown results in a local depression in wave heights, significantly modifying nearshore circulation patterns that enhance erosion in that area. The study highlights the advantage of exploring local erosion with a highly focused geomorphic and physical processes investigation, as well as a

broad, systemwide approach, to fully understand the variety of potential influences on local coastal behavior.

ACKNOWLEDGMENTS

We thank the U.S. Geological Survey (USGS) Mendenhall Postdoctoral Fellowship Program, the USGS Coastal and Marine Geology Program, and the U.S. Army Corps of Engineers, San Francisco District (especially Peter Mull), for funding this research. Mike Kellogg of the San Francisco Public Utilities Commission generously provided sediment data. The National Park Service provided research permits and other logistical support. Numerous other individuals contributed to the development and execution of this research effort. In particular, we thank Dan Hanes for his guidance and advice throughout the course of this investigation.

LITERATURE CITED

Allan, J.C. and Komar, P.D., 2006. Climate controls on US West Coast erosion processes. *Journal of Coastal Research,* 22(3), 511–529.

Atwater, B.F., Conrad, S.G., Dowden, J.N., Hedel, C.W., MacDonald, R.L., and Savage, W., 1979. History, landforms, and vegetation of the estuary's tidal marshes. *In:* Conomos, T.J. (ed.), *San Francisco Bay, the Urbanized Estuary*. San Francisco, California: Pacific Division of the American Association for the Advancement of Science, pp. 347–385.

Barnard, P.L. and Davis, R.A., Jr., 1999. Anthropogenic vs. natural influences on inlet evolution: west–central Florida. *In: Proceedings Coastal Sediments 1999 Conference* (Fire Island, New York), pp. 1489–1504.

Barnard, P.L. and Kvitek, R.G., 2010. Anthropogenic influence on recent bathymetric change in west–central San Francisco Bay. *San Francisco Estuary and Watershed Science,* 8(3), 13p.

Barnard, P.L. and Warrick, J.A., 2010. Dramatic beach and nearshore morphological changes due to extreme flooding at a wave-dominated river mouth. *Marine Geology,* 273(1–2), 131–148.

Barnard, P.L., Erikson, L.H., and Hansen, J.E., 2009. Monitoring and modeling shoreline response due to shoreface nourishment on a high-energy coast. *In:* da Silva, C.P. (ed.), *Proceedings of the 10th International Coastal Symposium, Lisbon, Portugal*. Journal of Coastal Research, Special Issue No. 56, pp. 29–33.

Barnard, P.L., Hoover, D., and Hansen, J.E., 2011. Nearshore bathymetric evolution on a high-energy beach during the 2009–10 El Niño winter. *In:* Wang, P., Rosati, J.D., and Roberts, T.M. (eds.), *Coastal Sediments '11, Proceedings of the 7th International Symposium on Coastal Engineering and Science of Coastal Sediment Processes* (Miami, Florida, American Society of Civil Engineers), pp. 1390–1403.

Barnard, P.L., Hanes, D.M., Rubin, D.M., and Kvitek, R.G., 2006. Giant sand waves at the mouth of San Francisco Bay. *Eos Transactions of the American Geophysical Union*, 87(29), 285, 289.

Barnard, P.L., Eshleman, J.L., Erikson, L.H., and Hanes, D.M., 2007a. Coastal Processes Study at Ocean Beach, San Francisco, CA: Summary of Data Collection 2004–2006. U.S. Geological Survey Open-File Report 2007-1217, 165p, http://pubs.usgs.gov/of/2007/1217/ (accessed December 20, 2011).

Barnard, P.L., Hanes, D.M., Lescinski, J., and Elias, E., 2007b. Monitoring and modeling nearshore dredge disposal for indirect beach nourishment, Ocean Beach, San Francisco. *In:* Smith, J.M. (ed.), *Coastal Engineering 2006, Proceedings of the 30th International Conference* (San Diego, California), Volume 4, pp. 4192–4204.

Barnard, P.L., Erikson, L.H., Hansen, J.E., and Elias, E., 2009. The Performance of Nearshore Dredge Disposal at Ocean Beach, San Francisco, California, 2005–2007. U.S. Geological Survey Open-File Report 2008-1347, 93p, http://pubs.usgs.gov/of/2008/1347/ (accessed December 20, 2011).

Barnard, P.L., Allan, J., Hansen, J.E., Kaminsky, G.M., Ruggiero, P., and Doria, A., 2011. The impact of the 2009–10 El Niño Modoki on U.S. West Coast beaches. *Geophysical Research Letters,* 38(L13604), 7p.

Barnard, P.L., Erikson, L.H., Rubin, D.M., Dartnell, P., and Kvitek, R.G., 2012. Analyzing bedforms mapped using multibeam sonar to determine regional bedload sediment transport patterns in the San Francisco Bay coastal system. *In:* Li, M., Sherwood, C., and Hill, P. (eds.), *International Association of Sedimentologists' Special Publication Book on Shelf Sedimentology*, Special Publication 44 of the International Association of Sedimentologists (IAS), pp. 273–294.

Battalio, R.T. and Trivedi, D., 1996. Sediment transport processes at Ocean Beach, San Francisco, CA. *In: Proceedings of the 25th International Conference on Coastal Engineering* (Orlando, Florida, American Society of Civil Engineers), pp. 2691–2707.

Benedet, L. and List, J.H., 2008. Evaluation of the physical process controlling beach changes adjacent to nearshore dredge pits. *Coastal Engineering,* 55, 1224–1236.

Booij, N., Ris, R.C., and Holthuijsen, L.H., 1999. A third-generation wave model for coastal regions. 1. Model description and validation. *Journal of Geophysical Research,* 104(C4), 7649–7666.

Bridges, M.H., 1995. Analysis of the Processes Creating Erosional Hot Spots in Beach Nourishment Projects. Coastal & Oceanographic Engineering Program, University of Florida, Gainesville, UFL/COEL-95/030, 135p.

Bromirski, P.D., Miller, A.J., Flick, R.E., and Auad, G., 2011. Dynamical suppression of sea level rise along the Pacific Coast of North America: indications for imminent acceleration. *Journal of Geophysical Research: Oceans,* 116(C07005), 13p.

Bruno, M.S., Yavary, M., and Herrington, T.O., 1998. The influence of a stabilized inlet on adjacent shorelines: Manasquan, New Jersey. *Shore & Beach,* 66(2), 19–25.

Capiella, K., Malzone, C., Smith, R., and Jaffe, B., 1999. Sedimentation and Bathymetry Changes in Suisun Bay (1867–1990). U.S. Geological Survey Open-File Report 99-563.

Cayan, D.R., Bromirski, P.D., Hayhoe, K., Tyree, M., Dettinger, M.D., and Flick, R.E., 2008. Climate change projections of sea level extremes along the California coast. *Climate Change,* 87(Suppl. 1), S57–S73.

Conomos, T., 1979. Properties and circulation of San Francisco Bay water. *In:* Conomos, T. (ed.) *San Francisco Bay: the Urbanized Estuary*. San Francisco, California: Pacific Division, American Association for the Advancement of Science, pp. 47–84.

Dallas, K. and Barnard, P.L., 2009. Linking human impacts within an estuary to ebb-tidal delta evolution. *In:* da Silva, C.P. (ed.), *Proceedings of the 10th International Coastal Symposium, Lisbon, Portugal*. Journal of Coastal Research, Special Issue No. 56, pp. 713–716.

Dallas, K. and Barnard, P.L., 2011. Anthropogenic influences on shoreline and nearshore evolution in the San Francisco Bay coastal system. *Estuarine, Coastal and Shelf Science,* 92(1), 195–204.

Davis, R.A., Jr. and Barnard, P.L., 2000. How anthropogenic factors in the back-barrier influence tidal inlet stability: examples from the Gulf Coast of Florida, USA. *In:* Pye, K. and Allen, J.R.L. (eds.), *Coastal and Estuarine Environments: Sedimentology, Geomorphology and Geoarchaeology*. London, United Kingdom: London Geological Society, pp. 293–303.

Davis, R.A., Jr. and Barnard, P.L., 2003. Morphodynamics of the barrier-inlet system, west–central Florida. *Marine Geology,* 200, 77–101.

Davis, R.A., Jr. and Fox, W.T., 1981. Interaction between wave- and tide-generated processes at the mouth of a microtidal estuary: Matanzas River, Florida (USA). *Marine Geology,* 60, 49–68.

Dean, R.G., Liotta, R., and Simón, G., 1999. Erosional Hot Spots. Coastal & Oceanographic Engineering Program, University of Florida, Gainesville, UFL/COEL-99/021, 60p.

El Banna, M.M. and Frihy, O.E., 2009. Human-induced changes in the geomorphology of the northeastern coast of the Nile Delta, Egypt. *Geomorphology,* 107, 72–78.

Elias, E.P.L. and van der Spek, A.J.F., 2006. Long-term morphodynamic evolution of Texel Inlet and its ebb-tidal delta (the Netherlands). *Marine Geology,* 225, 5–21.

Eshleman, J.L., Barnard, P.L., Erikson, L.H., and Hanes, D.M., 2007. Coupling alongshore variations in wave energy to beach morphologic change using the SWAN wave model at Ocean Beach, San Francisco, CA. *In: 10th International Workshop on Wave Hindcasting and Forecasting* (Oahu, Hawaii), Paper F4, 20p.

Fan, H., Huang, H., and Zeng, T., 2006. Impacts of anthropogenic activity on the recent evolution of the Huanghe (Yellow) River Delta. *Journal of Coastal Research,* 22, 919–929.

Fregoso, T.A., Foxgrover, A.C., and Jaffe, B.E., 2008. Sediment Deposition, Erosion, and Bathymetric Change in Central San Francisco Bay: 1855–1979. U.S. Geological Survey Open-File Report 2008-1312, 46p.

Frihy, O.E. and Komar, P.D., 1993. Long-term shoreline changes and the concentration of heavy minerals in beach sands of the Nile Delta, Egypt. *Marine Geology,* 115(3–4), 253–261.

Gibbs, R.J., 1972. The accuracy of particle size analyses utilizing settling tubes. *Journal of Sedimentary Petrology,* 42, 141–145.

Gilbert, G.K., 1917. Hydraulic-Mining Debris in the Sierra Nevada. U.S. Geological Survey Professional Paper 105, 154p.

Hanes, D.M. and Barnard, P.L., 2007. Morphological evolution in the San Francisco bight. *In:* Lemckert, C.J., (ed.), *Proceedings of the 9th International Coastal Symposium, Queensland, Australia*, Journal of Coastal Research, Special Issue No. 50, pp. 469–473.

Hansen, J.E. and Barnard, P.L., 2010. Sub-weekly to interannual variability of a high-energy shoreline. *Coastal Engineering,* 57(11–12), 959–972.

Hansen, J.E., Elias, E., List, J.H., and Barnard, P.L., 2011. A numerical model investigation of the formation and persistence of an erosion hot spot. *In:* Wang, P., Rosati, J.D., and Roberts, T.M. (eds.), *Coastal Sediments '11, Proceedings of the 7th International Symposium on Coastal Engineering and Science of Coastal Sediment Processes* (Miami, Florida, American Society of Civil Engineers), pp. 1769–1782.

Hapke, C.J., Reid, D., and Richmond, B., 2009. Rates and trends of coastal change in California and the regional behavior of the beach and cliff system. *Journal of Coastal Research,* 25(3), 603–615.

Hapke, C.J., Reid, D., Richmond, B.M., Ruggiero, P., and List, J., 2006. National Assessment of Shoreline Change: III. Historical Shoreline Changes and Associated Coastal Land Loss along the Sandy Shorelines of the California Coast. U.S. Geological Survey Open-File Report 2006-1219, 79p.

Hapke, C.J., Lentz, E.E., Gayes, P.T., McCoy, C.A., Hehre, R., Schwab, W.C., and Williams, S.J., 2010. A review of sediment budget imbalances along Fire Island, New York: can nearshore geologic framework and patterns of shoreline change explain the deficit? *Journal of Coastal Research,* 26(3), 510–522.

Hicks, D.M., Hume, T.M., Swales, A., and Green, M.O., 1999. Magnitudes, spatial extent, time scales and causes of shoreline change adjacent to an ebb-tidal delta, Katikati Inlet, New Zealand. *Journal of Coastal Research,* 15(1), 220–240.

Holthuijsen, L.H., Booij, N., and Ris, R.C., 1993. A spectral wave model for the coastal ocean. *In: Proceedings of the 2nd International Symposium of Ocean Wave Measurement and Analysis* (New Orleans, Louisiana), pp. 630–641..

Jabaloy-Sánchez, A., Lobo, F.J., Azor, A., Bárcenas, P., Fernández-Salas, L.M., Díaz del Río, V., and Pérez-Peña, J.V., 2010. Human-driven coastline changes in the Adra River deltaic system, southeast Spain. *Geomorphology,* 119, 9–22.

Jaffe, B., Smith, R.E., and Torresan, L.Z., 1998. Sedimentation Changes in San Pablo Bay 1856–1983. U.S. Geological Survey Open-File Report 98-759.

Jones, B.M., Arp, C.D., Jorgenson, M.T., Hinkel, K.M., Schmutz, J.A., and Flint, P.L., 2009. Increase in the rate and uniformity of coastline erosion in Arctic Alaska. *Geophysical Research Letters,* 36(L03503), 5p.

Jones, I.S., 2011. Wave Driven Set-Up and Surf Zone Circulation at Ocean Beach. San Francisco, California: San Francisco State University, Master's thesis, 43p.

Keller, B.R., 2009. Literature review of unconsolidated sediment in San Francisco Bay and nearby Pacific Ocean Coast. *San Francisco Estuary and Watershed Science,* 7.

Konicki, K.M. and Holman, R.A., 2000. The statistics and kinematics of transverse sand bars on an open coast. *Marine Geology,* 169, 69–100.

Kraus, N.C. and Galgano, F.A., 2001. Beach Erosional Hot Spot: Types, Causes, and Solutions. Coastal and Hydraulics Engineering Technical Note, United States Army Corps of Engineers, ERDC/CHL CHETN-II-44.

Lesser, G.R., Roelvink, J.A., van Kester, J.A., and Stelling, G.S., 2004. Development and validation of a three-dimensional morphological model. *Coastal Engineering,* 51, 883–915.

MacMahan, J., 2001. Hydrographic surveying from a personal watercraft. *Journal of Surveying Engineering,* 127(1), 12–24.

Mateo, Z.R.P. and Siringan, F.P., 2007. Tectonic control of high-frequency Holocene delta switching and fluvial migration in Lingayen Gulf bayhead, northwestern Philippines. *Journal of Coastal Research,* 23, 182–194.

McNinch, J.E., 2004. Geologic control in the nearshore: shore-oblique sandbars and shoreline erosional hotspots, mid-Atlantic bight, USA. *Marine Geology,* 211(1–2), 121–141.

NOAA (National Oceanic and Atmospheric Administration), 2009. NOAA Shoreline Data Explorer. http://www.ngs.noaa.gov/newsys_ims/shoreline/index.cfm (accessed December 20, 2012).

Porterfield, G., 1980. Sediment Transport of Streams Tributary to San Francisco, San Pablo and Suisun Bays, California, 1909–66. U.S. Geological Survey Water-Resources Investigations 80-64, 92p.

Ris, R.C., Holthuijsen, L.H., and Booij, N., 1999. A third-generation wave model for coastal regions. II. Verification. *Journal of Geophysical Research,* 104(C4), 7667–7681.

Ruggiero, P., Kaminsky, G.M., Gelfenbaum, G., and Voigt, B., 2005. Seasonal to interannual morphodynamics along a high-energy dissipative littoral cell. *Journal of Coastal Research,* 21(3), 553–578.

Schoellhamer, D.H., 2011. Sudden clearing of estuarine waters upon crossing the threshold from transport to supply regulation of sediment transport as an erodible sediment pool is depleted, San Francisco Bay, 1999. *Estuaries and Coasts,* 34(5), 885–899.

Scripps Institution of Oceanography, 2011. The Coastal Data Information Program. Integrative Oceanography Division, San Diego, California. http://cdip.ucsd.edu (accessed December 20, 2011).

Shi, F., Svendsen, I.A., Kirby, J.T., and Smith, J.M., 2003. A curvilinear version of a quasi-3D nearshore circulation model. *Coastal Engineering,* 49, 99–124.

Shi, F., Kirby, J.T., Newberger, P.A., and Haas, K.A., 2005. NearCoM Master Program. Version 2005.4: User's Manual and Module Integration. Research Report 2005-10. Newark, Delaware: Center for Applied Coastal Research, University of Delaware.

Shi, F., Hanes, D.M., Kirby, J.T., Erikson, L., Barnard, P.L., and Eshleman, J., 2011. Pressure gradient–dominated nearshore circulation on a beach influenced by a large inlet-tidal shoal system. *Journal of Geophysical Research: Oceans,* 116(C04020).

Slagel, M.J. and Griggs, G.B., 2008. Cumulative losses of sand to the California coast by dam impoundment. *Journal of Coastal Research,* 24(3), 571–584.

Stauble, D.K., 1994. Evaluation of erosion "hot spots" for beach fill project performance. *In: Proceedings of the 7th National Conference on Beach Preservation Technology* (Tampa, Florida, Florida Shore and Beach Preservation Association), pp. 198–215.

Svendsen, I.A., Haas, K.A., and Zhao, Q., 2000. Quasi-3D Nearshore Circulation Model SHORECIRC: Version 2.0. Research Report. Newark, Delaware: Center for Applied Coastal Research, University of Delaware.

Vermeer, M. and Rahmstorf, S., 2009. Global sea level linked to global temperature. *Proceedings of the National Academy of Sciences,* 106(51), 21527–21532.

Wingfield, D.K. and Storlazzi, C.D., 2007. Variability in oceanographic and meteorologic forcing along central California and its implications on nearshore processes. *Journal of Marine Systems,* 68, 457–472.

Wright, L.D. and Coleman, J.M., 1972. Wave climate and the role of the subaqueous profile. *Science,* 176(4032), 282–284.

Wright, S.A. and Schoellhamer, D.H., 2004. Trends in the sediment yield of the Sacramento River, California, 1957–2001. *San Francisco Estuary and Watershed Science,* 2(2), 14p.